Contrasting Structural Morphologies of "Good" and "Bad" Footed Horses

Robert M. Bowker, VMD, PhD

Author's address: Department of Pathobiology and Diagnostic Investigation, Michigan State University, East Lansing, MI 48824.

1. Introduction

The equine foot has evolved from the third digit and, through years of evolution, has become elongated and strengthened. While this structure has become "strengthened" to support the weight of the horse, one might find major arguments from some people about what it really means to have a "strong foot." Usually, most discussions revolve around the term "good conformation," which includes several variables such as thick walled hooves that will resist drying and have "normal" growth qualities.[1,2] The sole should be thick enough to resist most external traumas as well as be shed normally. The bars should also be well developed along with the frog. Other descriptions include the alignment of the foot with the axis of the distal limb with a mediolateral and a craniocaudal balance, and are usually mentioned because any imbalance can affect foot flight and stride length, etc.[3] Although these descriptions are vague and can vary from horse to horse, most people acquainted with horses can appreciate and understand this concept of a "strong foot" or "good foot." However, these descriptions include only the external parts of the foot, specifically the visible structures, and little or no mention is ever made of the possibility that the internal structures of the foot may contribute to a concept of a "good foot." Additionally, internal foot structures that may contribute to a condition of a horse with a "bad foot" are not mentioned. The latter term is the opposite of the "good-footed" horse and merely refers to a horse that continues to have foot problems, or more specifically, because it relates to the present discussion, a horse that has a foot with chronic lameness problems. From our work over the past few years of dissecting, examining, and studying the feet of most breeds as well as the feet of horses from different parts of the United States, we have discovered that the structural composition of the equine foot differs from foot to foot, although the anatomy of the equine foot is virtually identical. This statement means that although the internal anatomy of the foot is identical in terms of foot structures, the composition varies considerably from foot to foot. It is this variation in structure that seems, at the very least, to contribute to those horses living their entire lives without any major foot problems, whereas other horses seem to have been born with chronic foot problems. Thus, we have simplistically defined a "good-footed" horse as one that lives well into their 20s or 30s without any chronic foot problems such as navicular syndrome, whereas the "bad-footed" horse

NOTES

is usually euthanized early in life or as a teenager because of a history of chronic foot problems. Some people will argue with such statements; however, these statements serve as a beginning for the purposes of this discussion. Although most people would agree that the conformation of the horse foot is influenced by genetic factors, we believe that the environment has an equal or perhaps even greater influence in determining the "degree of goodness or badness" in the foot, and thus, the relative incidence of chronic foot problems. Our definition of "conformation" of the horse foot refers to a "point in time," because we have discovered that the structures and the internal composition of the foot appear to continually change over time from the birth of the foal to the death of the aged horse. Furthermore, if you move a horse to a different environment, the foot will adapt and change to a greater degree. We believe that these changes are primarily caused by environmental influences, because the internal morphology of the foot of the same breeds of horses differ depending on the environment, use of the horse, extent of movement and exercise, and husbandry habits, to name a few examples. One might suggest that a "good-footed" horse will adapt to produce a "strong foot," whereas the "bad-footed" horse has either not been able to adequately adapt or has "mal-adapted," leading to chronic foot problems.

Although discussion of the potential environmental influences on the foot is not the specific purpose of this work, we believe that one can see hints of its influence. This work is focused on several areas of the foot—specifically, the palmar foot and the structures surrounding the distal phalanx. The hoof wall and its adaptable capabilities are discussed in another paper. However, although each is discussed separately, they all interconnect and interact with each other, because the foot functions as a unit rather than as a series of individual parts. The events and forces influencing the palmar foot will affect the distal phalanx and hoof wall, and vice versa. The foot gradually changes and adapts to the applied forces and loads within its environment to become "stronger," and thus, the internal structures change their shapes, structure, and even biochemical composition. However, some feet, depending on the environment, may not be able to change or adapt to the fullest extent to minimize the forces being loaded on the tissues. Although there are probably many possible reasons for this inability to adapt, the environment (husbandry practices, relative lack of movement or exercise, farrier and veterinary care, etc.) seems to be a major contributor to the lack of development or under development of the foot. The horse will potentially become the "bad-footed" horse.

2. Changes in the Palmar Foot and Its Structures: Thick Cartilages, Fibrocartilaginous Digital Cushions, and Increased Vasculature in "Good-Footed" Horses

The palmar foot consists of specific sensory detectors and several important structures functioning to support the foot and limb of the horses during stance and locomotion. They also provide propulsion during movement and aid in the dissipation of the energies generated during foot impact.[4–10] The structural support of the internal foot structures include the lateral or ungular cartilages, the digits cushion, and the extensive vascular network.[11–14]

While each of these structures are present in every foot, the morphology and tissue composition vary from foot to foot. This variation between feet can be seen even in the same horse, but it is seen more often in a large population of horses from different regions of the country and from different backgrounds of use.[12] Furthermore, the structural features and composition of the foot vary with age; although horses under 4–5 yr have a relatively similar structure, regardless of breed, older horses have wide variety in the structures of these tissues.[a] These differences among the feet of different horses may be responsible for the abilities of the foot to dissipate energy during ground impact as well as minimize stress on the foot tissues during stance. Awareness of the interaction and relation of these tissues to each other and the variation of their compositions from horse to horse is important for understanding how the foot dissipates energy during locomotion and how the palmar foot provides support for the bone, ligaments, and other tissues of the foot during stance. When these tissues are not well adapted and do not efficiently distribute the impact forces evenly during movement or the loads during stance, potential problems may arise that cause lameness because the tissues of these areas and other regions of the foot receive higher energy loads caused by the uneven or unbalanced distribution of the forces to the foot tissues.[6–8,10] As a result, certain foot tissues receive increased loads, which results in increased stress. Stress in tissues is defined as the load per unit area. A load applied to the foot with a small surface area will produce higher stress in the underlying tissues than an identical load applied to the foot with a greater surface area. The location where these loads are concentrated and the tissues which receive the loads are critical to maintaining a healthy foot because certain tissues are well adapted to energy dissipation and load support, whereas other tissues are not. The structural composition of a healthy foot will minimize the stress to the bone, connective tissue, hoof wall, and epidermal laminae, etc., and thus, minimize potential lameness conditions.[4–10] Furthermore, because the domestic horse spends considerable time standing in a stall or grazing in a pasture, one can appreciate that the structure of the

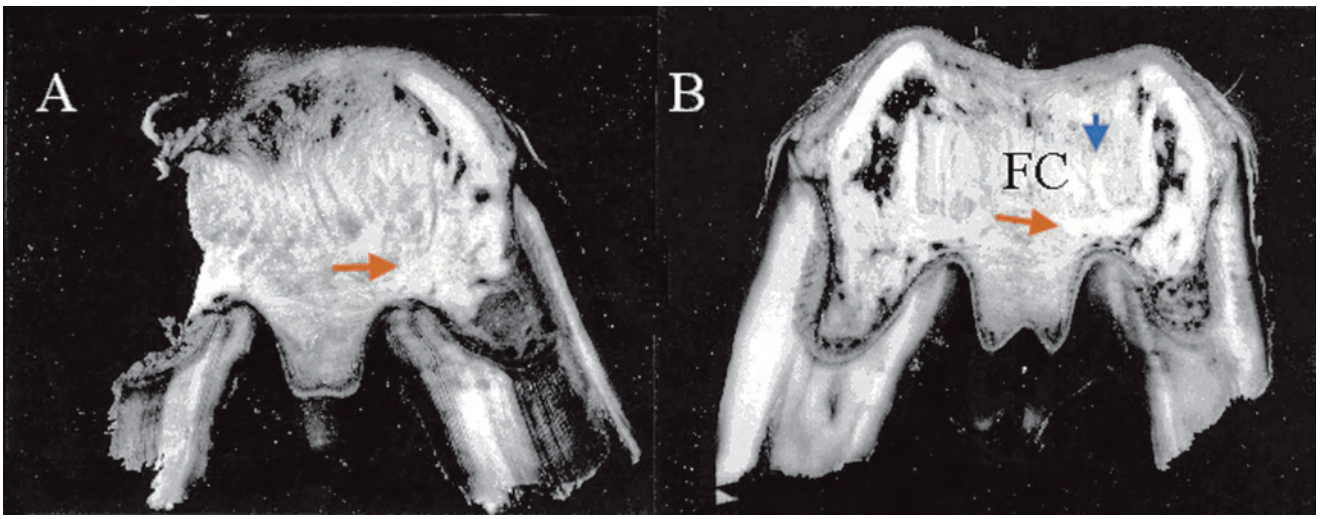

Fig. 1. Transverse sections through caudal part of foot illustrating the relation of the lateral cartilage and the axial projection to bars of sole. The axial projection (red arrows) does not extend as far toward midline in foot A with thinner lateral cartilage (0.475 in) as it does in foot B (0.678 in). Additionally, there is little fibrocartilage (FC) in digital cushion. There is also more extensive vascular filling of lateral cartilage B (black India ink area). Courtesy of *Am J Vet Res*.

palmar foot is important for support during these activities to minimize the weight or loads of the horse being shifted to other foot areas that are not designed to support the loads.[12–14,a]

The overall anatomy of the palmar foot has been well described.[11,14–16] However, these descriptions only discuss the foot in generalities and usually do not include the specific details that distinguish the structural anatomy of the "good-footed" horse from the foot of the "bad-footed" horse. The medial and lateral cartilages of the foot extend from the caudal edge of the distal phalanx to the bulbs of the heel in large, vertically oriented sheets.[11,14] Enclosed between these two sheets is the digital or plantar cushion, which extends from the toe ventral to the deep digital flexor tendon (DDFT) and along the solar surface of the distal phalanx.[11–14] Within the digital cushion, beginning at its dorsal edge, is the digital torus,[11] which emanates bands of fibrous tissue that radiate palmarly through the digital cushion.[12] Associated with the cartilage of the foot is an extensive venous vasculature that joins the venous network under the distal phalanx and that is associated with the dermis of the hoof wall and the coronet.[12,17]

3. The Cartilages of the Foot

The cartilages of the foot lie beneath the skin, corium, and coronary venous plexus. They are rhomboid-shaped with the convex surface facing the outside of the foot, whereas the concave surface is facing toward the midline of the digital cushion.[11,13,14] This description has historically been used in most texts for the anatomy of the lateral cartilages, regardless of whether the foot was from a horse with chronic foot problems or a horse that had no indication of any foot disease.[11,13,14,16] From early drawings of the internal anatomy of the foot,[11] we believe that such descriptions may have been from "bad-footed" horses obtained from abattoirs. These descriptions of the cartilages are as overly simplistic as those in the drawings. Many of the palmar structures are underdeveloped. As we will demonstrate, the morphological features of the lateral cartilages vary greatly from horse to horse in shapes and thickness, presence or absence of a fibrocartilaginous axial projection, and extent of the vascularity inside and outside of the cartilage.[a,12] We believe the variation of these morphological features to be mainly determined by environmental factors rather than by genetics, because the anatomy can vary considerable within the same breed of horse. Horses having many positive environmental factors seem to have "good" feet. Positive environmental factors include frog and sole pressure that stimulate or "exercise" the solar surface of the foot, with more exercise being more advantageous, and movement. In frontal sections cut perpendicular to the ground between the bulbs of the heels and the toe, the cartilages have a "C" or "L" shaped configuration (Fig. 1). The upright and the base part of the cartilage vary considerably in thickness among horses. The mean thickness of the upright part at the level of the navicular bone ranges from 0.5 to 2.0 cm in the adult horse weighing between 450 and 550 kg. The base part or axial projection of the "L" shaped cartilage varies in the thickness and in the distance it extends toward the midline, especially in the most palmar parts of the foot. The cartilages are thinnest at the heel region (0.45–1.3

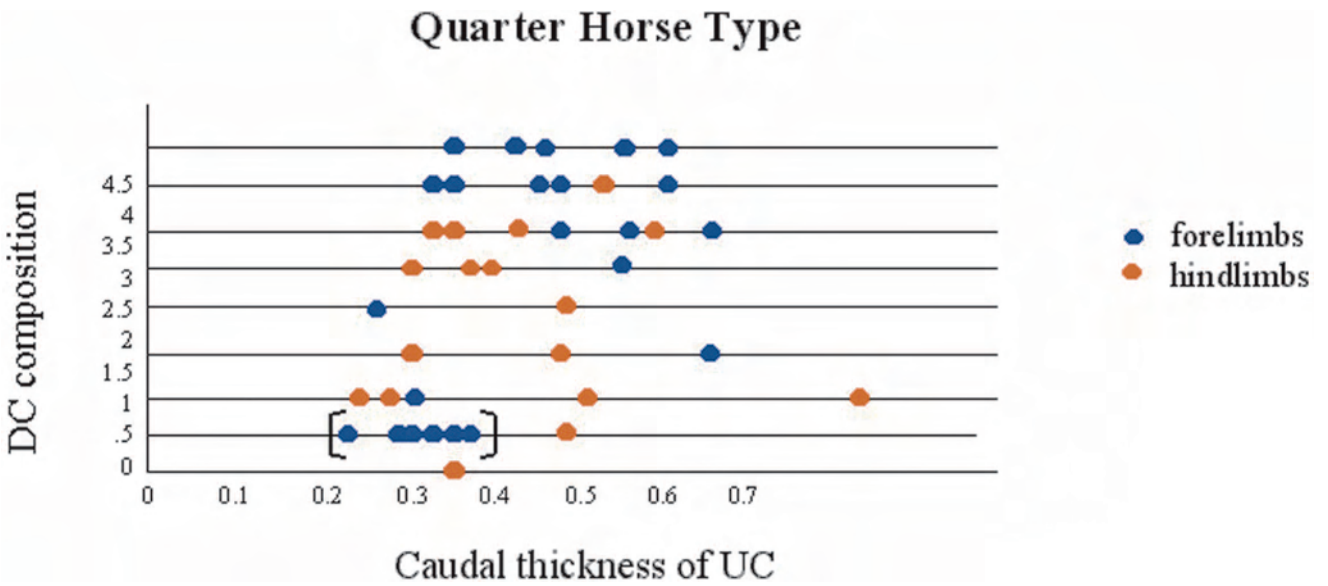

Fig. 2. Graph from small group of Quarter Horses (age > 5 yr) illustrating relationship between thickness of caudal third of lateral cartilage (UC) as measured with calipers to nearest 0.001 in and relative composition of digital cushion. The digital cushion of the forelimbs (blue) contain significantly more FC than the hind limb (red) from the same horse. The bracketed area indicates a group of navicular syndrome affected horses. Scale: (1) the digital cushion is all fat, elastic, proteoglycan, and collagen tissue, (2) digital cushion also contains some fibrous tissue but no FC, (3) some fibrocartilage is present as small granules, (4) extensive fibrocartilage present as large bundles and granules.

cm) but become thicker toward the distal phalanx (0.6–1.5 cm). When comparing the mean thickness of the lateral cartilages of the foot of the same horse, the cartilages for the forelimb are significantly thicker than those of the hind limb ($p < 0.05$) (Figs. 2 and 3).[12]

On the outside of the lateral cartilages are the extensive venous plexus, laminar dermis, and inner layer of the hoof wall. On the inside of the lateral cartilage, the base of the "L" shaped cartilage extends toward the midline of the digital cushion. The axial projection exists in the dorsal half of the lateral cartilage, because it attaches along the inside of the palmar process and the DDFT before the latter attaches along the semilunar line distally and the flexor surface proximally (being attached at a mean distance of 1.6 mm) (Fig. 4). The caudal half of the lateral cartilage has very little extension into the digital cushion. This general description of the axial projection appears in most young horses under 4–5 yr, including racing horses, whereas in older horses with "good feet," the more palmar cartilaginous base extends further into the substance of the digital cushion. Because it extends toward the midline of the foot, the cartilaginous axial projection overlies the epidermal ridges of the bars with many finger-like projections of fibrous bands extending into the substance of the digital cushion (Fig. 1). The fibrous bands will often fuse with the ones from the opposite side of the foot. These white bands of fibrous tissue are easily discerned from the surrounding yellowish mass of fat as well as the elastic and collagen fibers comprising the digital cushion. The relative thickness of the axial projection varies considerably in a proximal to distal direction from horse to horse. In the "good-footed" horse in its mid- to late 20s, the axial projection can be up to 5–8 mm thick, whereas in "bad-footed" horse, this projection is absent or may exist only as a thin sheet of fibrous tissue. In horses under 4–5 yr, the axial projection is not fully developed, is composed mainly of fibrous tissue with some fibrocartilage near the junction between the projection and the lateral cartilage, and is usually absent caudally. In foals and yearlings, it is only a thin sheet of fibrous tissue.

The lateral cartilage is primarily hyaline cartilage, and in horses older than 4–5 yr, the medial boundary begins to develop fibrocartilage (Fig. 3). On freshly sectioned specimens, the hyaline and fibrocartilage can easily be distinguished by the white and yellowish coloration of the respective cartilage. This development gradually creates a thickened lateral cartilage that can extend upward to more than 1.5 cm as a mean thickness along its length from the wings of the distal phalanx to the heels. Between the lateral cartilage and the DDFT, a fibrocartilaginous ligament becomes evident, which extends proximally to the level proximal to that of the navicular bone (Fig. 3). This robust ligament between the DDFT and the lateral cartilage is evident mainly in the "good-footed" horse, whereas in other horses, only thin fibrous connections are evident between these two sites. This

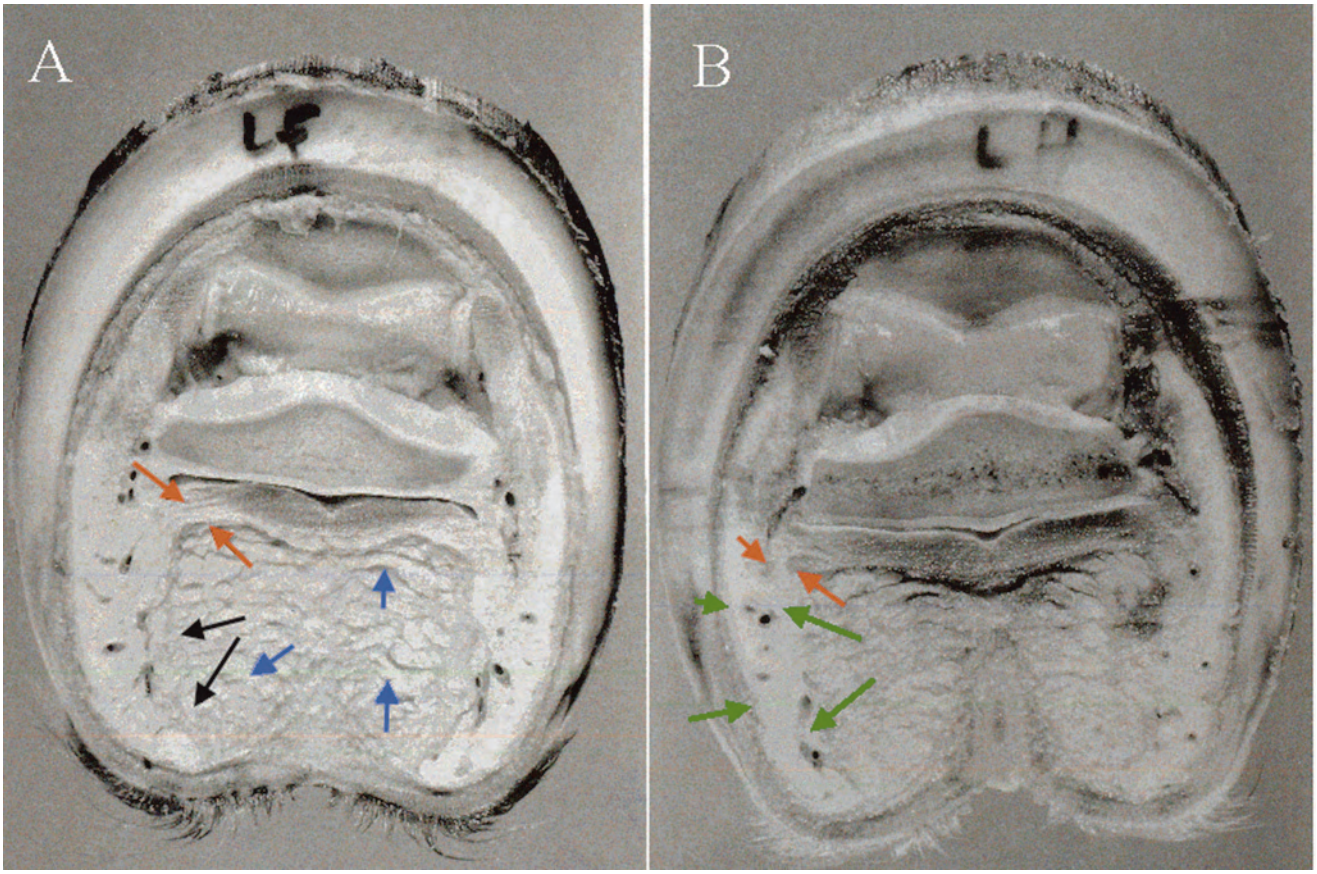

Fig. 3. Sections through level of navicular bone showing left front foot A and left hind foot B from same horse. Observe that the lateral cartilages are thicker in forelimb than in hind limb (green arrows). Also, observe that the ligament between the cartilage and the DDFT (red arrows) is thicker than in hind foot with latter being composed mainly of fibrous tissue. The blue arrow points out fibrocartilage in front foot. The lateral cartilage fuses along its axial surface with fibrocartilage of digital cushion (black arrows). Courtesy of *Am J Vet Res*.

ligament, when present, is thicker in the forelimb than that of the hind limb (Fig. 3).

Several ligaments attach the lateral cartilages to the bones of the digit and the navicular bone.[11,14,16] The chondroungular ligaments attach to the lateral cartilage along the palmar process. Interestingly, in those feet in which the lateral cartilages begins to ossify in a palmar direction, this ligament may eventually become enveloped within the newly formed bone and may not be very functional. The medial and lateral chondrocoronal ligaments attach the cartilage to the distal ends of the middle phalanx dorsally, whereas the collateral chondroungular ligaments attach the lateral cartilage to the angle of the distal phalanx. The paired chondrosesamoidean ligaments attach the axial surface of the cartilage to the navicular bone. A pair of elastic ligaments extend between the proximal phalanx and the edge of the lateral cartilages of the foot, and they are most prominent in larger horses such as the draft breeds. Within the digital cushion, fiber tracts are present, radiating from the connective tissue ventral to the attachment of the DDFT (digital torus) through the digital cushion. These bundles of collagen fibers and fibrous tissues become the fibrocartilage present within the digital cushion of the "good-footed" horse.

Each hoof cartilage is perforated by vascular foramina, but the number varies depending in part on the thickness of the lateral cartilage. For example, in the "good-footed" horse with thick lateral cartilages, the relative number of vascular channels at the proximal level of the foot (navicular bone) may exceed 25–30 channels per two lateral cartilages (Fig. 5A). On the other hand, in the "bad-footed" horse, the number of vascular channels at that same level is usually zero, but may be up to three to five channels per two lateral cartilages (Fig. 5B). Within the vascular channels is a large central vein with a rich network of microvessels, termed veno-venoanastomoses (Fig. 5, C and D). Within the tubular core of the lateral cartilage that contains the vein, small microvessels can be seen to exit the large vein and course for considerable distance be-

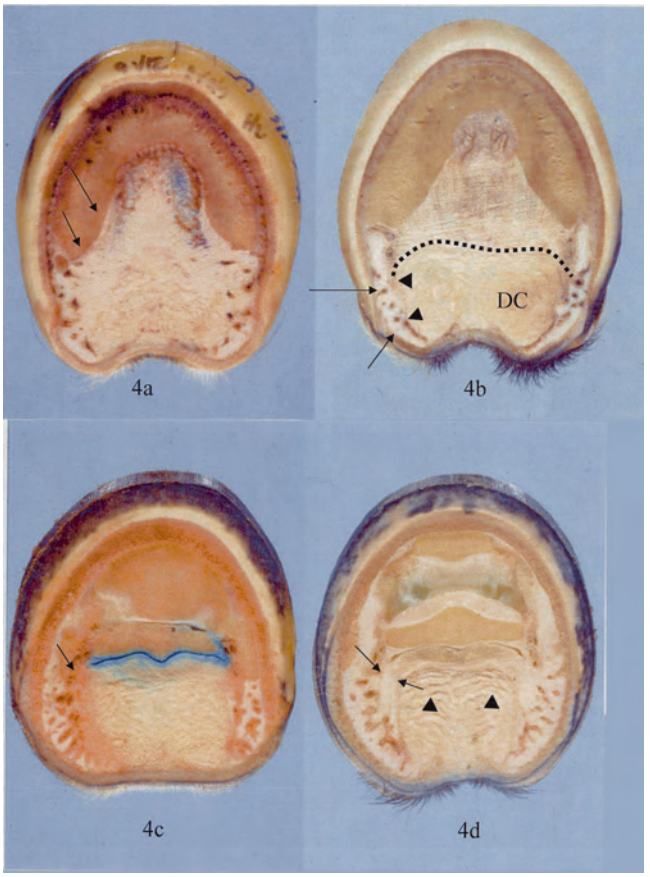

Fig. 4. Sections showing foot and its structure in four horses. (A) Section from hind foot showing lateral cartilage and axial projection extending along distal phalanx (black arrows) toward semiluminar line. Note caudal part of digital cushion is yellow, indicating fat and elastic tissue and little or no fibrocartilage. (B) Forefoot distally showing relatively thin lateral cartilage (between arrows and arrowheads) and yellow fat and elastic digital cushion (DC) (caudal to dotted line). (C) At level of navicular bone, in forefoot with relatively thicker lateral cartilage and blood vessels within the lateral cartilage as well as along axial surface, but a digital cushion with mainly fat, elastic, and collagen and no fibrocartilage. Arrow indicates fibrous, but not fibrocartilaginous, ligament between the lateral cartilage and the DDFT. Blue stain marks navicular bursa. (D) Foot has thick lateral cartilage and fibrocartilage (arrowheads) in digital cushion. Black arrows indicate fibrocartilaginous ligament between the cartilage and the DDFT.

fore re-entering the vein without supplying the walls of the lateral cartilage tube or the parenchyma with either the cartilage or digital cushion. Interestingly, in feet perfused with an Indian ink solution, frozen, and sectioned, there is a greater filling of the vasculature of the thickened lateral cartilages than in those feet with thin lateral cartilages (compare with Fig. 1, A and B). These findings suggest that there may be more small networks of microvessels within thicker lateral cartilages than in the feet having thin lateral cartilages. At the distal level of the lateral cartilage, many more vascular channels are evident, and they become fewer at a more proximal level such as that of the navicular bone. The enclosed veins then coalesce proximal to the lateral cartilage into a venous plexus before uniting to form the medial and lateral palmar digital vein.[16–21] Figure 6 illustrates a three-dimensional drawing of a foot with thin lateral cartilage versus a foot with a thicker lateral cartilage.

4. Digital Cushion

The digital cushion consists of a meshwork of collagen and elastic fiber bundles with proteoglycans and small areas of adipose tissue, which lie between the

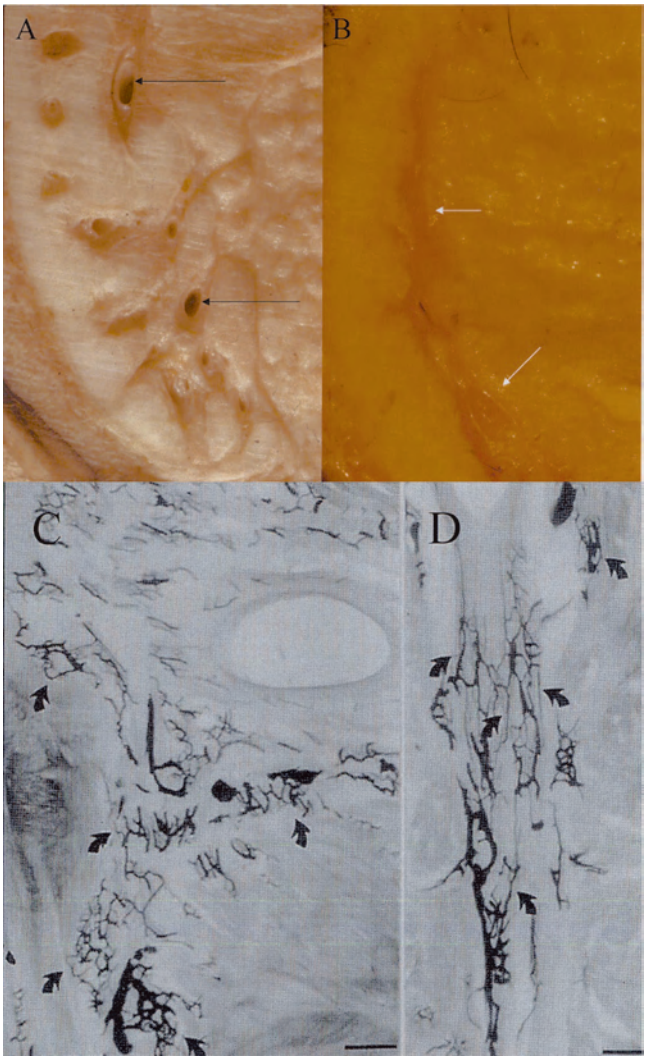

Fig. 5. Views at level of navicular bone showing thick lateral cartilage (A) with several vascular channels (arrows) within lateral cartilage and a thin lateral cartilage (B) where vasculature is axial to lateral cartilage (white arrows). The microvessels (arrows, Bar: 100 microns) filled with India ink can be seen in cross section (C) and in a longitudinal section (D). Courtesy of *Am J Vet Res*.

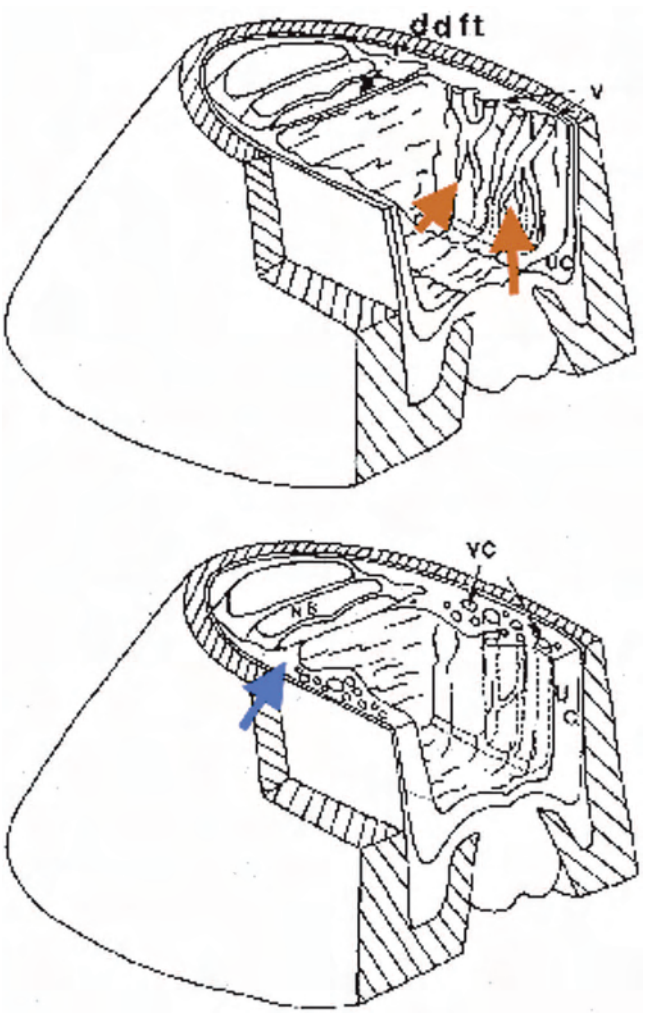

Fig. 6. Three dimensional composite drawings of the support structure of the ungual cartilage (UC) or lateral cartilage in horses with thin (top) versus thick (bottom) portions of the UC. Notice that venous vessels exit the axial surface of the UC sooner in feet with thin UC (red arrows) than in feet with thick UC (B). The ligamentous attachment (blue arrow) from the UC to the DDFT is typically thicker and more cartilaginous in feet with thick UC. NB, navicular bone; UC, veins inside vascular channels.

lateral cartilages of the foot and above the frog and epidermal bars. This tissue extends toward the toe of the foot under and near the distal attachment of the DDFT and the solar surface of the distal phalanx. This composition of the digital cushion is present in most young horses, regardless of their breed and work amount as foals, yearlings, and even race horses (Quarter Horses, Thoroughbreds and Standardbreds have this type of foot until 4–5 yr).[a] Beyond this youthful foot, the internal structure may begin to change from the isolated collagen bundles to ones that contain varying amounts of fibrocartilage throughout the digital cushion. With stimulation of the frog and solar surface of the foot, the fibrocartilage forms to fill the digital cushion, starting distally and progressing proximally beyond the level of the navicular bone. In these feet, the isolated collagen bundles begin to coalesce and form fibrocartilage and thereby thicken between the developing lateral cartilages and midline of the digital cushion (Fig. 3A). The lateral cartilages in these feet will become thicker when the axial surface of the lateral cartilage develops fibrocartilage. At this point, the lateral cartilages are composed of hyaline cartilage abaxially, while the inner edge begins to form fibrocartilage. This change gives the appearance that the lateral cartilage is growing toward the midline of the foot, because the fibrocartilage of the lateral cartilage and the digital cushion unite to form a significant structural support for the palmar foot. Simultaneously, the connective attachments between the lateral cartilage and the DDFT also thicken to become a robust fibrocartilaginous ligament (Fig. 3A). This structural reorganization of the palmar foot seems to occur over a long period of time with proper stimulation. The blood supply to the digital cushion is small, because only small capillaries are evident within the parenchyma of the digital cushion; however, there are two large arteries that pass through the digital cushion that supply the vasculature of the frog.

From the above descriptions of the palmar foot and the dissections of many feet, several assessments can be made. Firstly, in most young horses under the age of 4–5 yr, there are few differences in the internal foot structures regardless of the breed of horse.[a] After this age, definite differences begin to become noticeable. The lateral cartilage becomes gradually thicker and the digital cushion becomes filled with fibrocartilage along with changes in the microvasculature in some horses and breeds, although other horses' feet remain virtually unchanged from the youthful foot. Certain breeds, i.e., Arabians and Standardbreds, do seem to have a higher percentage of fibrocartilaginous distal cushions and thick lateral cartilages earlier in the years after the age of 4–5 yr than other breeds. In other words, we also believe that most "good footed" horses develop this trait after 4–5 yr with "stimulation and exercise," whereas most "bad-footed" horsed remain structurally underdeveloped and do not develop the robust palmar foot at 4–5 yr. We have no evidence that the extensive fibrocartilage in a "good footed" horse will regress to fat, elastic, and collagenous bundles. With this gradual development of an interactive structural composite of the lateral cartilages and the digital cushion, the apparent health of the palmar foot improves with the aging of the horse. These horses have less clinically evident chronic foot problems, such as navicular syndrome, than those horses without these internal fibrocartilaginous morphologies of the palmar foot. We also

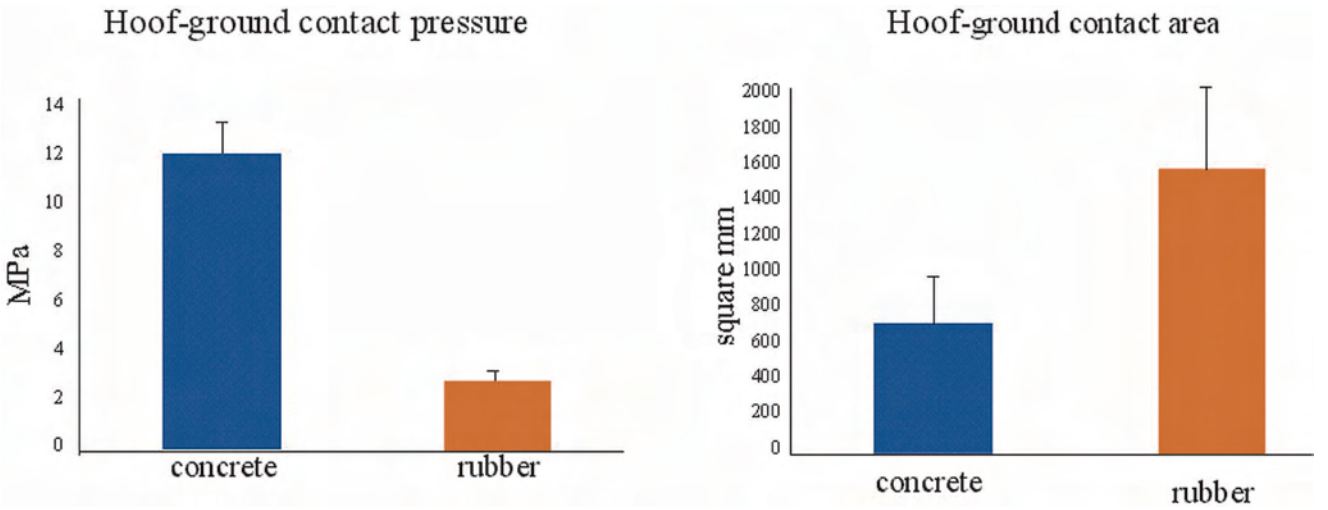

Fig. 7. Graphs showing mean contact pressure (left) and hoof contact area (right) of six horses when they stood on concrete and hard rubber. Left panel: The contact pressure is highest on hard, non-deformable surfaces (concrete) (mean = 12 MPa), whereas on hard rubber, contact pressure is reduced to less than one-quarter. Right panel: The contact area of horses on concrete is approximately one-half of that on rubber. Together both graphs show that the foot has high stress (load per area) on hard surfaces (concrete) versus those that are deformable surfaces (hard rubber).

expect an increase in the vasculature within the palmar foot. Although these observations may suggest that the palmar foot will gradually develop the fibrocartilaginous palmar foot while the horse ages, these internal foot changes do not occur with age alone but with proper foot "exercise and stimulation." Age is not the critical factor in developing a fibrocartilage palmar foot, because horses that do not have "sufficient palmar foot stimulation" have only thin lateral cartilages and digital cushions composed of fat, elastic, and isolated collagen bundles with very little fibrocartilage. Such horses include brood mares and other "pasture-ornament" horses with minimal movement and foot stimulation during their lifetime. These fibrocartilaginous changes seem to develop when the palmar foot becomes stimulated with the frog and bars on the ground and the solar surface increasing the surface area for load distribution.

The question arises: are there ways to attempt the improvement of the structure of the palmar foot? More specifically, can the foot be "exercised" to create an increased area of sole and frog support? Such a process may potentially improve the functioning of the foot, because the increased area of foot contact will reduce the load that is placed on the tissue, and thus, the stress on the tissue. This finding is illustrated using pressure sensitive film (Fig. 7). The horses' feet have a smaller surface area when imprinted on a hard (cement) surface than when the same feet are placed on very firm rubber (durometer number 9) (Fig. 7, A [left] and B [right]). If the load placed on the foot is expressed as load per unit area, the load on the tissues (stress) decreases significantly when standing on firm rubber or other deformable environmental surface compared with cement. These findings are consistent with hoof impaction on different surfaces.[22] Measurable changes in the external solar foot (widened foot, changed angle of the bars, increased size and growth of the frog, reduced arching of the sole, etc.) can be observed in the unshod horse within 3–6 wk after shoe removal (Fig. 8, A and B). By altering the environment and increasing the surface contact area of the palmar foot, we believe that the palmar foot will become "strengthened," because it becomes an active participant during movement of the horse.

The structural organization of the lateral cartilages, digital cushion, and enclosed vasculature[18–21] suggests that they play a significant role in the dissipation of the impact during the foot's contact with the ground.[12] The pressure theory suggests that the frog pushes upward into the digital cushion at ground contact to force the lateral cartilages outward. On the other hand, the depression theory emphasizes the downward movement of the pastern into the digital cushion, which in turn forces the lateral cartilages outwardly.[10,13,15] However, neither theory can explain the large negative pressure present within the deep areas of the digital cushion during both stance and locomotion.[9] A hydraulic mechanism is created by the anatomical arrangement of the lateral cartilages, vasculature, and digital cushion in conjunction with the neuromodulation of the microvasculature (see below), which provide for the transfer of impact energies from the foot structures of the hoof to the cartilage and fluids within the foot.[12] This "energy transfer" system is one prime function of these tissues and determines

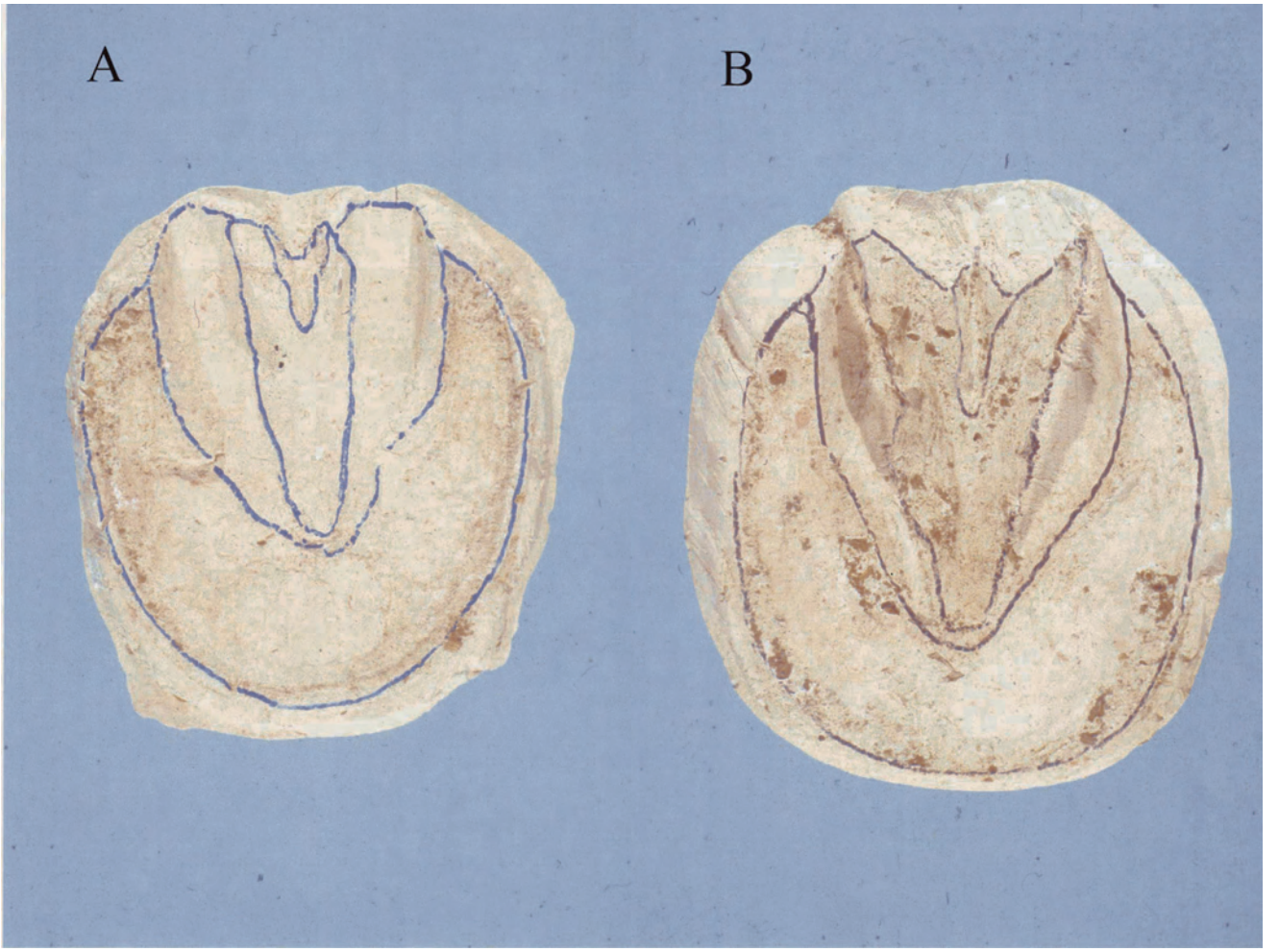

Fig. 8. Plaster of Paris casts obtained from clay imprints showing the gradual but typical changes one observes when shoes are removed and the horse is barefoot. The same foot (A) was molded 6 wk later in B. The distance between the apex of the frog and toe decreased, the solar surface of the foot widened 4–6 mm, the angle of bars increased (less vertical), and the frog enlarged.

their arrangement. At impact, the blood is forced through the microvasculature. This provides a resistance to the flow of the blood within the microvessels, and thus, reduces the amount of the impact high frequency energies that will be transferred to the bone and ligamentous parts of the foot. The negative pressure in the palmar foot permits the rapid refilling of the vasculature before the next foot fall.[9,12] In those horses with thick lateral cartilages that enclose a greater number of small vessels and a fibrocartilaginous digital cushion, more energy will potentially be dissipated by the hydraulic mechanism than in those feet that have thin lateral cartilages with a relatively small number of microvessels and a digital cushion devoid of fibrocartilage. In the latter foot with an undeveloped hydraulic system, less energy will be dissipated, resulting in a greater percentage of the impact energies being potentially transferred to the bones and ligaments of the foot. These initial impact energies and frequency vibrations inductions are considered to be the most destructive to the tissues within the foot.[23–26] The fibrocartilage content of the digital cushion is crucial to energy dissipation, because the fibrocartilage contains proteoglycans that aid in energy dissipation. Elastic tissue, as a biomechanical tissue, acts merely as a spring, presumably returning the tissues of the foot to their original position after the foot leaves the ground.

As discussed above, the shape of the foot influences the development of the thick lateral cartilages and the composition of the digital cushion. In the "good-footed' horse, initial heel contact is important along with having both the frog and bars making ground contact. At initial heel contact during locomotion, specific sensory receptors can be activated promoting full extension at the forelimb (Fig. 9).[27] In addition, the characteristics of the frog include being large and firm beyond the superficial dehydrated layer and often

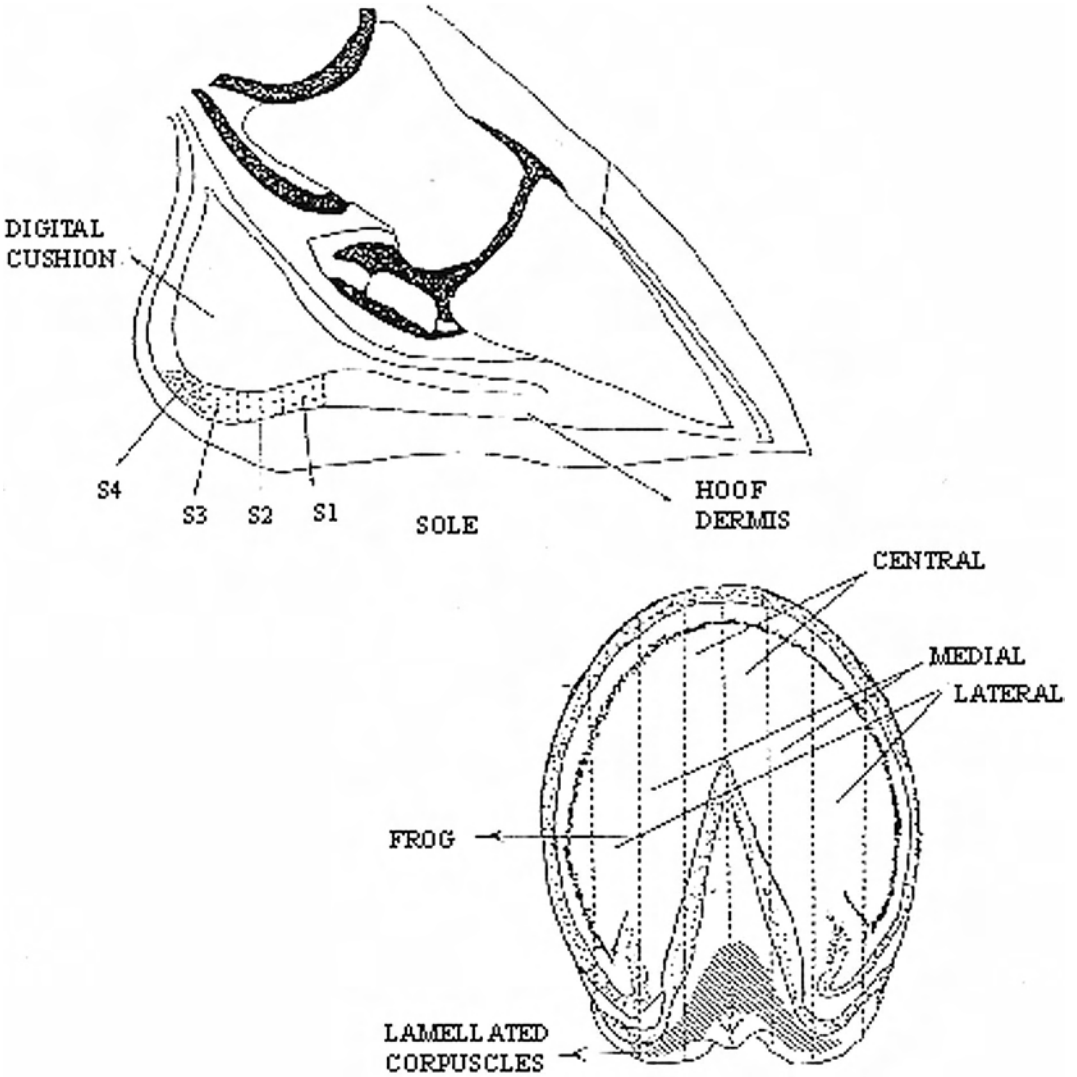

Fig. 9. Schematic illustrations of a midsagittal and ventral view of the equine foot. In the sagittal view, the four zones of the sole (S^{1-4}) represent the locations of the lamellated corpuscles with the relative density being indicated by the dots in each zone of S^{1-4}. In the most caudal zone (S^4), lamellated receptors were most frequently observed on tissue sections compared with the other zones (S^{1-3}). The ventral view of the foot represents the area obtained from longitudinal strips of central, medial, and lateral solar dermis that were examined on sections for the Pacinian type of receptor. The lamellated corpuscles were only observed on sections obtained from the line shaded area. Courtesy of *Am J Vet Res.*

having a distinct cushion (i.e., swelling 3–4 cm caudal to apex) and shallow sulcus. The bars are angled at approximately 60° rather than upright or vertical. We believe that this structure encourages the continued stimulation of the palmar foot with the development of the thick cartilages and fibrocartilaginous digital cushion. In the problematic foot, the frog usually does not make ground contact, or, if it does contact the ground, it lacks any significant firm (fibrocartilage) substance of the tissue. The bars are usually more upright rather than having an oblique angle with the ground surface (contracted foot). In these feet, the frog and solar foot have very little ground contact; thus, the load support is mainly around the perimeter of the foot. In feet that have a long toe or an under-run heel, the area of ground contact is usually further forward under the palmar process of the distal phalanx rather than underneath the lateral cartilages themselves. In these latter types of feet, less energy is absorbed by the hydraulic mechanism in the palmar foot, resulting in a greater percentage of the impact energy being transferred to the bones and ligaments of the foot. Such an inefficient energy dissipation system may gradually produce lameness conditions in the foot.

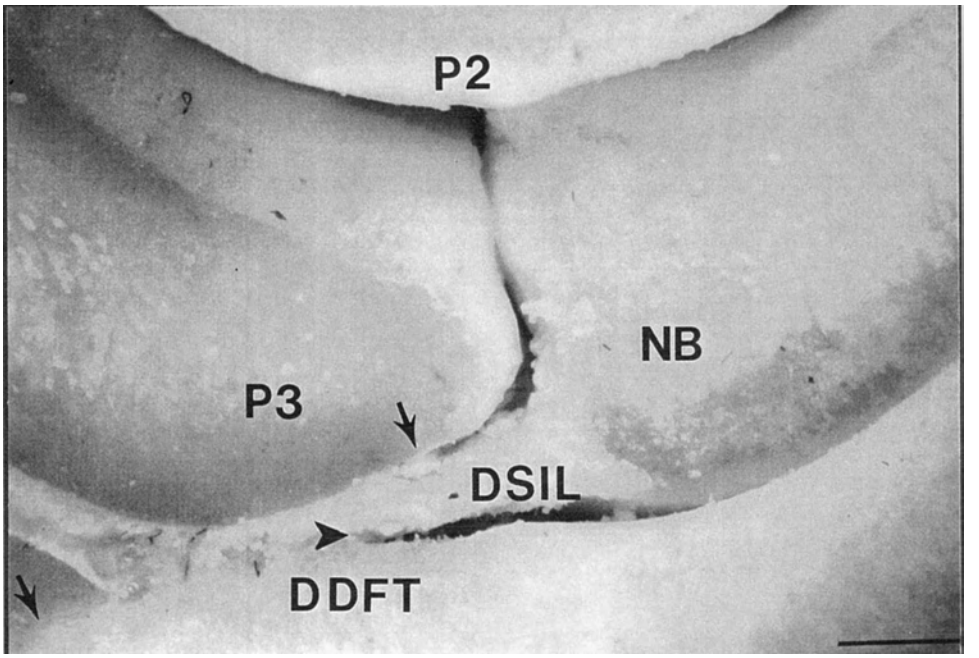

Fig. 10. Low magnification photograph of a parasagittal section of healthy foot, revealing the insertion of the DDFT and the DSIL on the distal phalanx (P3). Notice the area of the insertion (arrows) that the navicular bursa often does not extend to the P3 (arrowhead). P2, middle phalanx; NB, navicular bone.

5. Changes in the Anatomy of the Intersection and the Distal Phalanx: Stressed Areas in the "Bad-Footed" Horse

Although the continued success of any performance horse is dependent on being free of lameness conditions, several lameness conditions remain ambiguous in terms of the initiating causes and pathogenic events leading to the onset of clinical signs. Navicular syndrome, with its generally insidious onset, slow progression, bilateral lameness, and variety of radiographic features, suggests that there may be several potential causes for this condition. Several ideas have been proposed including (1) pressure of the DDFT against the flexor cortex of the navicular bone, (2) vascular insults, and (3) alterations in bony remodeling.[28–34] The vascular cause has largely been rejected, because most studies do not find any significant evidence of ischemic bone or inability to reproduce the syndrome by occluding the blood supply to the navicular bone.[32] The other hypotheses remain viable options, including the possibility of age-related degenerative processes occurring in these lame horses.[29–33] Our laboratory has suggested that much of the problem may occur in the distal phalanx and at the intersection of the insertion sites of the distal sesamoideum impar ligament (DSIL) and the DDFT.[35–37] Changes caused by increased stress as well as changes in the underlying bone of the distal phalanx occur at these sites (Fig. 10). We have hypothesized that progressive stress in the tissues of this region of the foot may significantly contribute to the onset of clinical signs associated with navicular syndrome. The macroscopic and microscopic morphology of the insertion sites of the DSIL and the DDFT appear to be more complex than those of other ligaments within the equine digit.[35] Furthermore, many of the neurovascular structures course through this region when they pass to the distal phalanx and solar corium and to the palmar foot, creating a critical site or "bottleneck" for potential problems affecting other areas of the foot. The DSIL-DDFT insertion site consists of regular dense connective tissue fiber bundles separated by penetrating loose connective septa, (Figs. 11 and 12) which contain an abundance of small vascular networks, elastic tissue, arteriovenous complexes, and nerves and their receptors (Fig. 11). The arteriovenous complexes form an interesting glomus type of vascular network within the DSIL and the dorsal half of the DDFT, which appear to be surrounded by other epithelial-like cells (Fig. 13). Their location within the DSIL and the DDFT suggests that they may serve one or more functions such as sensory detection of mechanical stresses and/or maintaining optimal hydration of the DSIL and the DDFT.[38] During movement and stance of the horse, considerable and sudden pressure changes will most likely occur in this region and could potentially restrict or enhance blood flow to the surrounding tissues, both of which may deleteriously affect the health of the perfused tissues.[39–41] The sensory detection function would ensure ade-

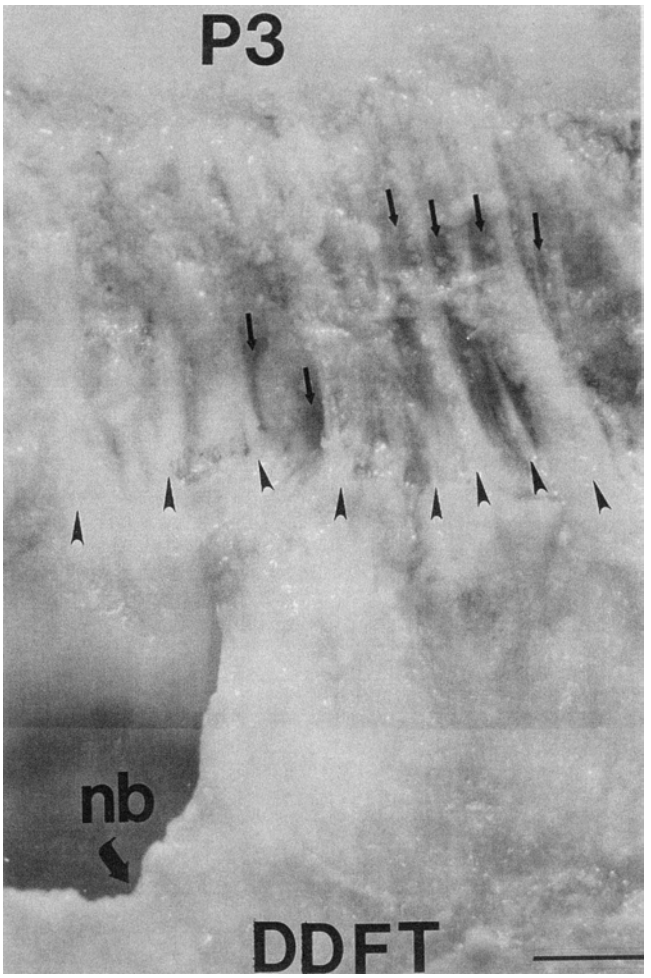

Fig. 11. In this photograph, the section is cut parallel to the surface of the ground. The navicular bursa (NB; large arrow) is between the DDFT and the navicular bone. Notice that the collagen bundles (arrowheads) can be seen at the insertion of the fusion of the DDFT and the DSIL along with connective tissue septa (small arrows) containing the microvasculature and sensory nerve fibers. Calibration mark is 1 mm. P3, distal phalanx. Courtesy of *Am J Vet Res*.

quate arterial blood flow to the navicular bone, because the majority of the arterial supply courses through this region[42] and moves to the distal phalanx. It also maintains proper venous drainage from these regions[21] and the palmar aspect of the foot for energy dissipation.[12]

While the vasoconstrictive nature of the arteriovenous complexes are under sympathetic noradrenergic control,[43–46] a potent vasodilatation mechanism exists under the control of neuropeptides including the tachykinin substance P (SP).[47–49] SP, neurokinin A (NKA), and calcitonin gene-related peptide (CGRP) have been shown to be present in the sensory nerve fibers that course through the DSIL and the dorsal half of the DDFT and pass into the distal phalanx and the navicular bone.[50] Although these peptides within the nerve fibers serve a sensory function, they also serve an efferent function. When the nerve fibers are activated, the neuropeptides are released from the nerve terminal into the surrounding tissues[48,51] and act through a nitric oxide mechanism to produce vasodilation.[52,53] This mechanism provides another avenue for the nervous system to aid and regulate the movement of fluids, ions, metabolites, and other compounds within the tissue environment.[47,48,54] Such fluid movements will maximize the efficiency of energy transfer, thereby minimizing peak pressure changes that damage tissues. Furthermore, the equine digit analogs of SP have been shown to be potent vasodilators even in the presence of high concentrations of norepinephrine (unpublished observation). In addition, documented peripheral release of all three peptides has been shown to promote inflammation, vasodilatation, and edema formation, and stimulate leukocytes to release their contents.[47,51,54,55] The sites where SP receptors are located can be visualized using receptor autoradiography in which the tissues are bathed in a radiolabeled ligand–in this case, radioactive SP is used.[56] Within the equine foot, the SP receptors are localized on the microvasculature and the arteriovenous complexes within the DSIL and the DDFT (Figs. 14 and 15).[b,56]

In the "bad-footed" horse, this intricate neurovascular network is damaged or disrupted functionally by the stresses and tissue damage occurring within the DSIL and the dorsal half of the DDFT. In comparing the examinations of the navicular horses and the control specimens, the tachykinin receptors present on the small vasculature within this region of the foot seem to be destroyed because they cannot be detected using receptor autoradiography.[b] These findings suggest that the neural control of the microvasculature supplying blood and venous drainage to and from the navicular bone and the distal phalanx has been compromised and the microvasculature has been destroyed.[b42–57] As a result, there may be insufficient arterial blood supply to these areas; thus, it can be observed that there is navicular bone erosion within the formation of synovial fossae and/or areas of both degenerative and regenerative bone within the navicular bone itself.[28,29,32,33] These same adaptive changes may also be occurring on the distal phalanx and at the intersection, because there is an increased size of the vascular channels in the flexor surface supplying the distal phalanx through the insertion site of the DSIL.[b]

Biomechanical stress to the different foot tissues may, in part, be responsible for chronic foot problems, or at the very least, may exacerbate some lameness conditions. The actual determination of the forces and loads applied to the hoof or the foot have been examined by a variety of different methodologies,[4,40,41,58-60] and each one contributes to our understanding of the foot. The in vivo meth-

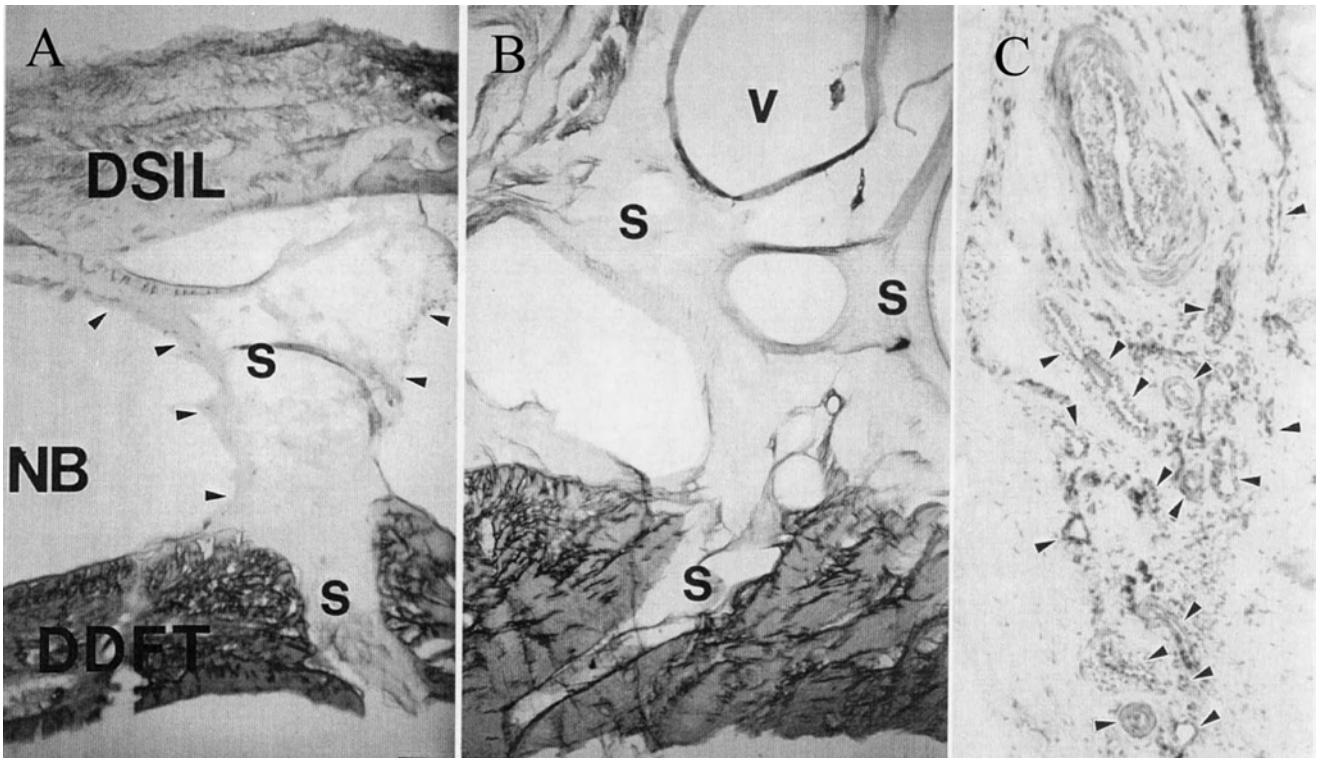

Fig. 12. Photomicrographs of tissue sections in the region of the insertion of the DSIL and the DDFT on the distal phalanx. (A) Distal outpocketings of the navicular bursa (NB) between the DSIL and the DDFT are separated by thin sheets of connective tissue septa (S). The septa extend from the DSIL into the dorsal half of the DDFT (arrowheads). (B) Section obtained near the distal phalanx, notice more small vessels (V) are evident within the septa (S). (C) Histological sections were obtained from the same area as B. Notice many more microvessels with arteriovenous complexes (AVC; arrowheads) are apparent within the septal sheets. A and B are not stained. C is stained with trichrome stain.

ods[4,41,58,60] usually examine the loads applied externally to the foot in contrast to the in vitro studies that enable explorations of the inner workings of the foot.[37,40,41] However, each method of examining the foot has certain shortcomings. As our primary interest has been examining the distal phalanx and its anatomy and determining how the potential stresses may affect this region of the foot, we have studied the distal interphalangeal (DIP) joint using pressure sensitive film. The "limb" was positioned in three different angulations to simulate the "normal' stance of the horse and the positions during movement of the digit.[37] When the three digital bones are aligned and the navicular bone is non–weight-bearing (angle of solar surface digit is 30° in relationship to the first phalanx), the position represents a standing horse limb. During movement at or near the breakover of the foot, the solar surface of the foot remains positioned on the ground, while the limb is moving forward or dorsiflexing the digit (this position is 0° with the solar surface being perpendicular to applied load). At this position, both the distal phalanx and the navicular bone are supporting the weight of the horse. An intermediate position of 15° reflects the loads on the digit between the "normal" stance and the breakover of the foot, such as a "broken back" hoof pastern axis (Fig. 16).

When the digit is placed in a testing machine and the loads are applied to the digit with the pressure sensitive film between the different joints, (between the middle and the distal phalanx, the middle phalanx and the navicular bone, and the navicular bone and the distal phalanx) the contact pressures, contact areas, and thus, loads (pressure $\times$ area) between the different joints can be studied and determined. Not unexpectedly, the minimum loads applied to the joints between the navicular bone and the distal phalanx, and the navicular bone and the middle phalanx were during the simulated "normal" position, when the navicular bone is a non–weight-bearing structure during the alignment of the digital bones. During the simulated "breakover" position, the loads increased significantly between the middle phalanx and the navicular bone, and between the navicular bone and the distal phalanx when the contact area of the joint increased (Fig. 17). It is during this positioning of the bones that the navicular bone becomes a weight-bearing structure and the loads are applied to the suspensory ligaments at the navicular bone. These biomechanical findings

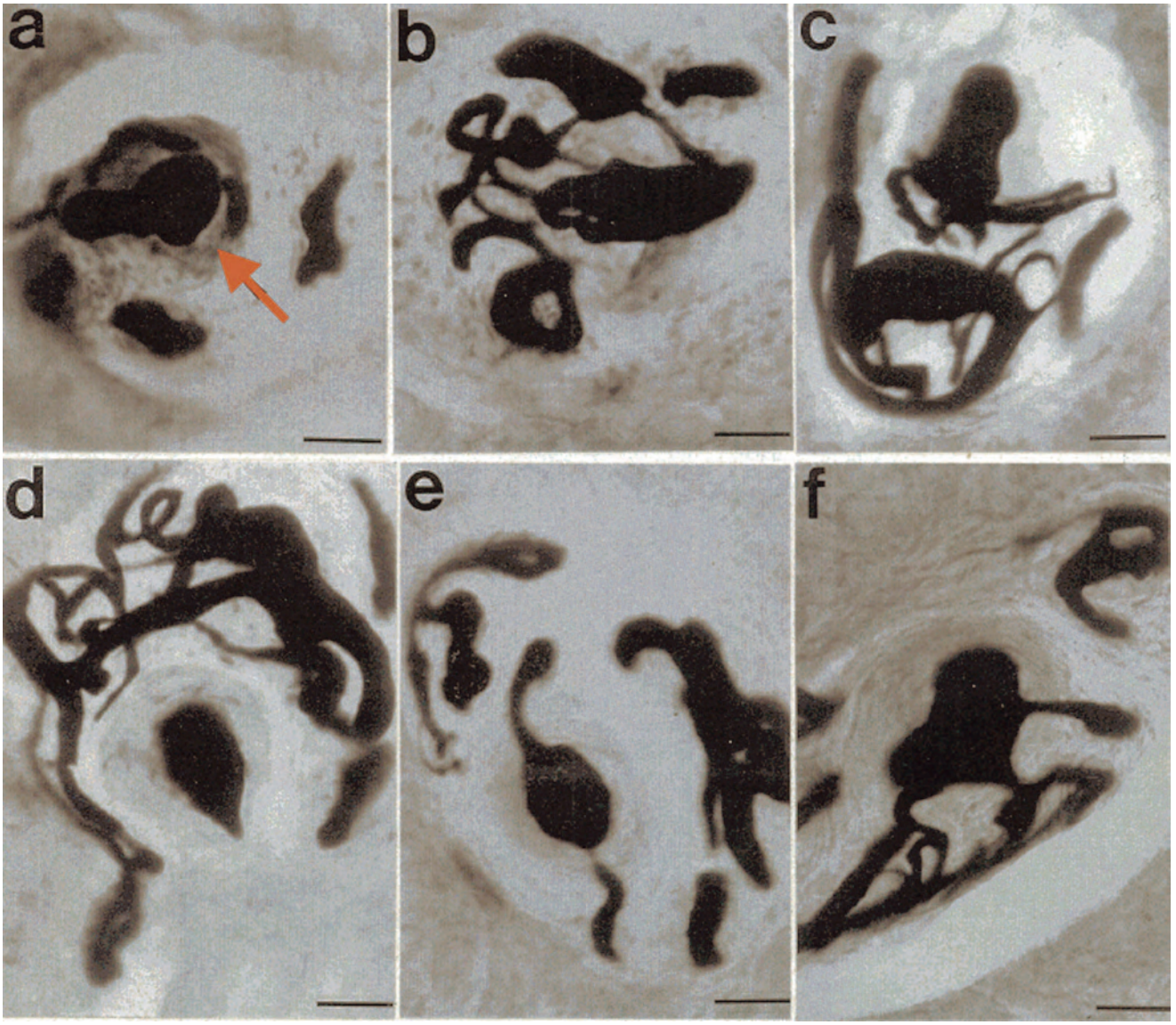

Fig. 13. Photomicrographs of serial tissue sections (90 ìm thick) in the regions of the DSIL-DDFT insertion on the distal phalanx from a healthy foot reveals the typical arteriovenous complexes (AVC) after infusion of vasculature with India ink. In A, India ink-filled vasculature can be tracked from the central vessel (red arrow) through a tortuous capillary network (B-D, especially C and D) and then to where it joins a large central vessel (E and F). Stain: H&E. Bars = 80 ìm.

are also correlated with the histological findings observed in an additional 54 horses with an age range of 2–29 yr. They included 11 Standardbreds, 16 Quarter Horses, 6 Arabians, 5 Thoroughbreds, and 16 mixed breeds; all horses had no clinical evidence of problems associated with the foot or digit.[35]

These feet were cut parasagittally and prepared for histological examination using H&E and safranin O with fast green stain. The areas of interest included the ligamentous attachments of the DSIL and the DDFT to the flexor surface of the distal phalanx and the navicular bone and the palmar half of the distal phalanx, including the articular surfaces between the navicular bone and the distal phalanx, and between the middle and distal phalanx. The safranin O dye stains proteoglycans in articular cartilage and fibroblasts capable of producing proteoglycans. The stain shows as a bright red coloration of the cartilage matrix and around the perimeter of the nucleus of a fibroblast that can extend throughout the cell and extracellular matrix. The production of proteoglycans by fibroblasts indicates the connective tissues are adapting to compressive stresses and are responding to the loads applied to the feet and distal limbs during the life of the horse. Although this morphological indicator of stress merely shows that the tissues have adapted and responded to the loads applied to the feet, we

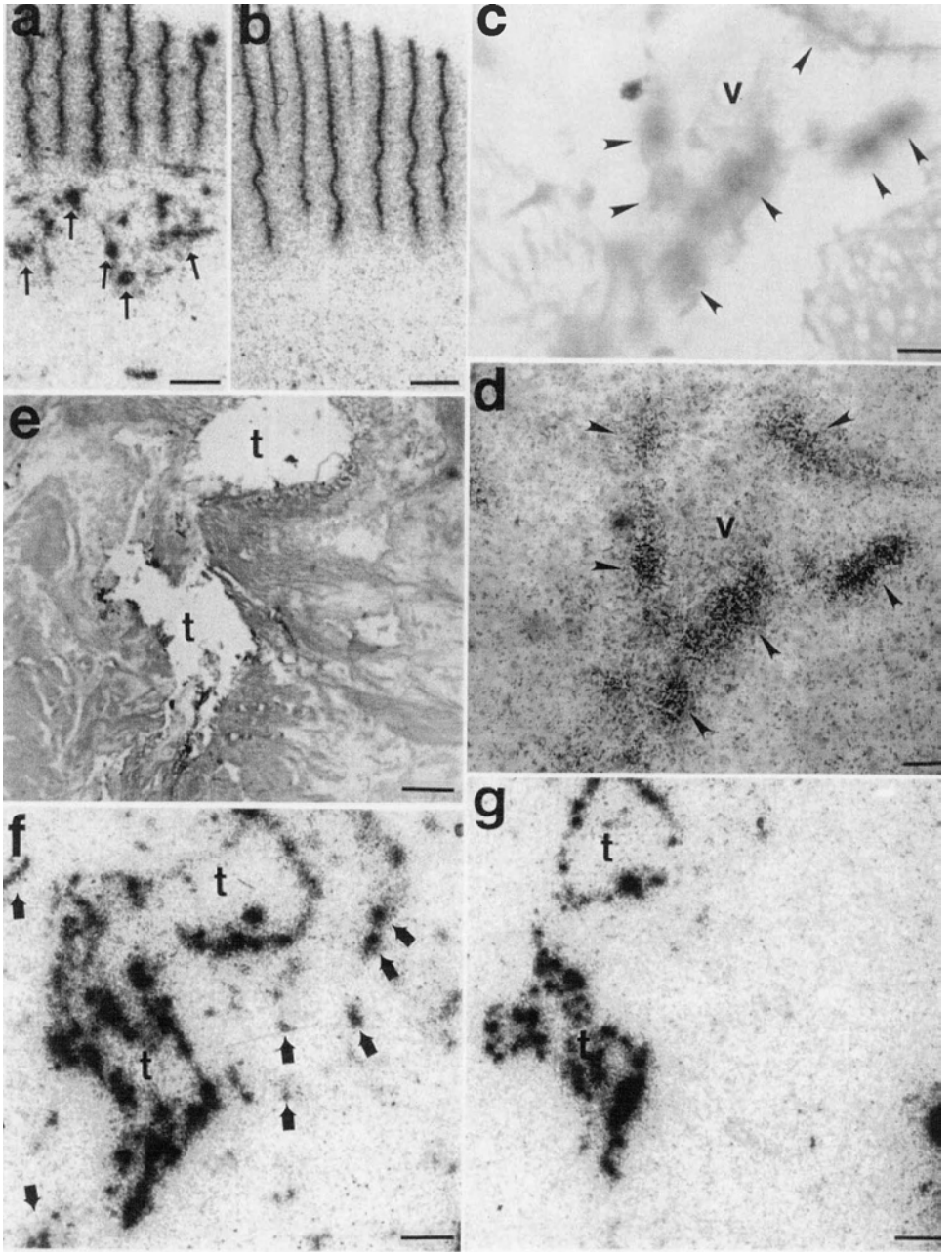

Fig. 14. Photomicrographs of radiographic film and tissue sections reveal binding sites of radioactive SP in the dorsal hoof wall (A and B) and the DSIL-DDFT insertion (C-G). Panel A: Total binding of radioactive SP can be seen as dark areas of accumulations of silver grains (arrows) overlying isolated dermal microvessels. Panel B Nonspecific binding of radioactive SP after incubation with 1 ìmol of unlabeled SP revealing that there was not any specific binding evident over microvessels in the dermis, whereas the primary epidermal (keratinized) laminae has non-specific labeling. Panel C: The tissue section of the DSIL was superimposed on the corresponding radiographic film, with the focal plane being the tissue section. Specific binding of radioactive SP is evident over the arteriovenous complexes (AVC) in the septa of the DSIL (arrowheads), whereas a small arteriolar vessel (v) has little or scant SP binding. Panel D: The same superimposed section and film as panel C, but the plane of focus is for the silver grains on the radiographic film. Notice that the silver grains (arrowheads) are concentrated over the AVC rather than over the larger vessel (v). Panels E and F: Tissue sections (panel E) and autoradiogram (panel F) of the DSIL reveal specific binding of radioactive SP over isolated microvessels (arrows), whereas the tear (t) in the tissue section creates non-specific binding of radioactive SP. Panel G: Non-specific binding on an adjacent tissue section incubated in radioactive SP; non-labeled SP is seen clearly around the perimeter of a tear (t) in the autoradiogram. Bars = 1 mm. For all photomicrographs of the tissue sections, light methylene blue and eosin Y stain was used. For the autoradiograms, the actual radiograph is shown. Courtesy of *Am J Vet Res*.

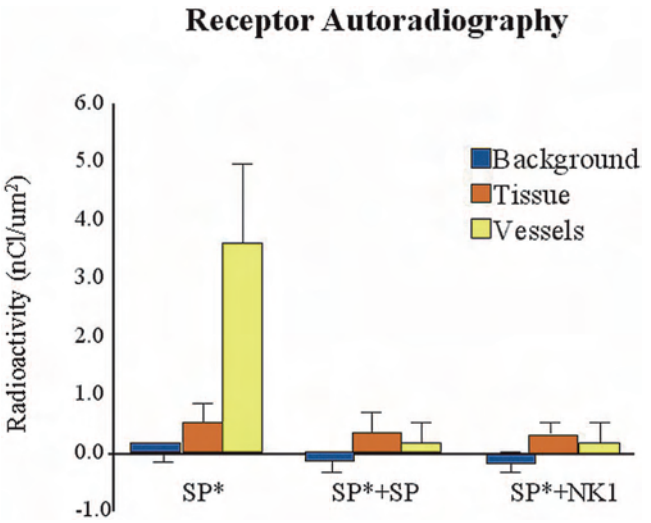

Fig. 15. Graph illustrating that virtually all SP receptors are neurokinin 1(NK1) receptors, and they are localized on microvessels, especially arteriovenous complexes. Results (mean ± SEM) show specific binding of radioactive SP (SP*) in the vessels (microvessels and AVC; yellow bar), tissues (red bar), and slide (background; blue bar). Incubations used SP* alone, SP* and unlabeled SP, and SP* and an excess of NK1 agonist. Courtesy of *Am J Vet Res*.

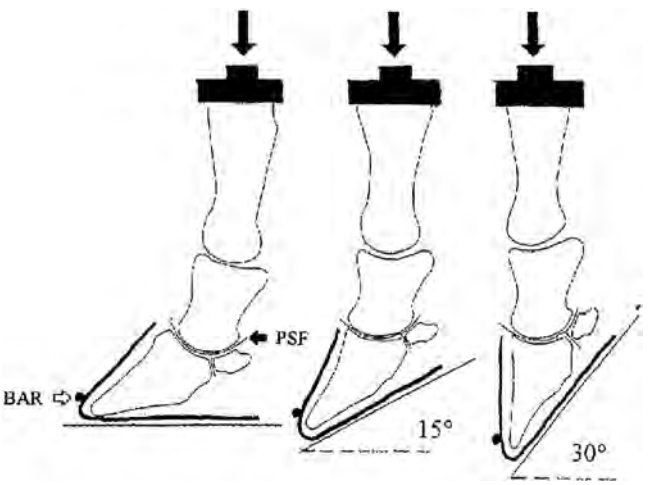

Fig. 16. Schematic drawings indicating relative stance positions of digits at the three flexion angles of 0° (left), 15° (middle), and 30° (right). For each flexion angle, the load was applied through the first phalanx (large solid arrow) with the solar surface of the hoof positioned on the metal plate of a material testing machine. The retaining bar at the toe (BAR; open arrow) prevented forward movement of the foot. Pressure-sensitive film (PSF; small solid arrow) was positioned in the joints between respective bones to determine contact forces. Courtesy of *Am J Vet Res*.

use the stain to roughly approximate the amount of adaptive compressive stress response that the tissues have undergone. In other words, a small amount of stress resulting in a few stained cells

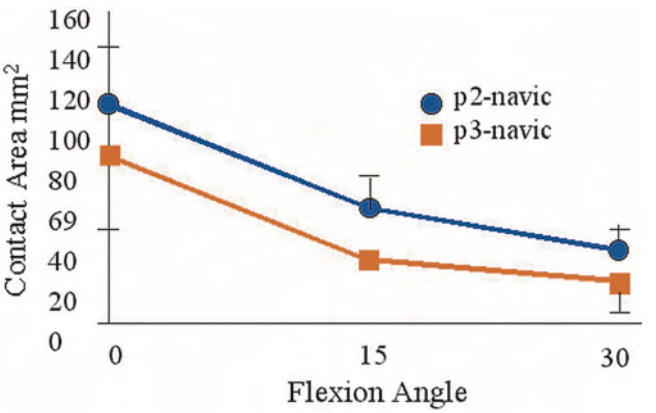

Fig. 17. Changes in values (mean ± SD) for contact area between the middle phalanx and navicular bone (circle) and between the navicular bone and distal phalanx (square) at flexion angles of 0°, 15°, and 30°. Notice that there was a significant ($p \leq 0.05$) increase in contact area, and thus, load at 0° compared with values at 15° and 30°. Courtesy of *Am J Vet Res*.

histologically may be seen in a "healthy and sound-footed" horse and would not be considered pathological. However, with greater stress applied to these same tissues as a result of either greater loads or inadequate tissue adaptation, the fibroblasts and other cellular constituents produced greater quantities of proteoglycans, which is indicated by detection of greater numbers of proteoglycan-producing cells that extend throughout the tissue and the extracellular matrix. These cells may be transformed into chondrocytes and produce cartilage, both of which can extend considerable distances from the attachments of the DSIL and the DDFT on the distal phalanx. These markers can be used for proteoglycan production and comparison of the different sections from many specimens. One can obtain an impression of the stress responses in tissues, which can be seen in clinically sound horses, and compare it to that seen in the lame horse suffering from navicular syndrome. We have observed a range of proteoglycan production from little or no staining to extensive staining. The staining patterns for proteoglycans were subjectively graded as (1) slight to no evidence of staining, (2) moderate staining, and (3) extensive staining for proteoglycan. This third category indicated that many more cells extended more than 1–2 mm beyond the insertion of the DSIL and the DDFT. In most instances, category three included staining of the connective tissues for distances greater than 1 cm from the attachment site along the proximal extent of the DSIL and the DDFT.

At the insertion site on the distal phalanx, the transition from the connective tissue to the ligament/tendon consists of typical distinct regions of these types of tissues (Fig. 18).[61–63] The fibroblasts were slender and spindle shaped and became more

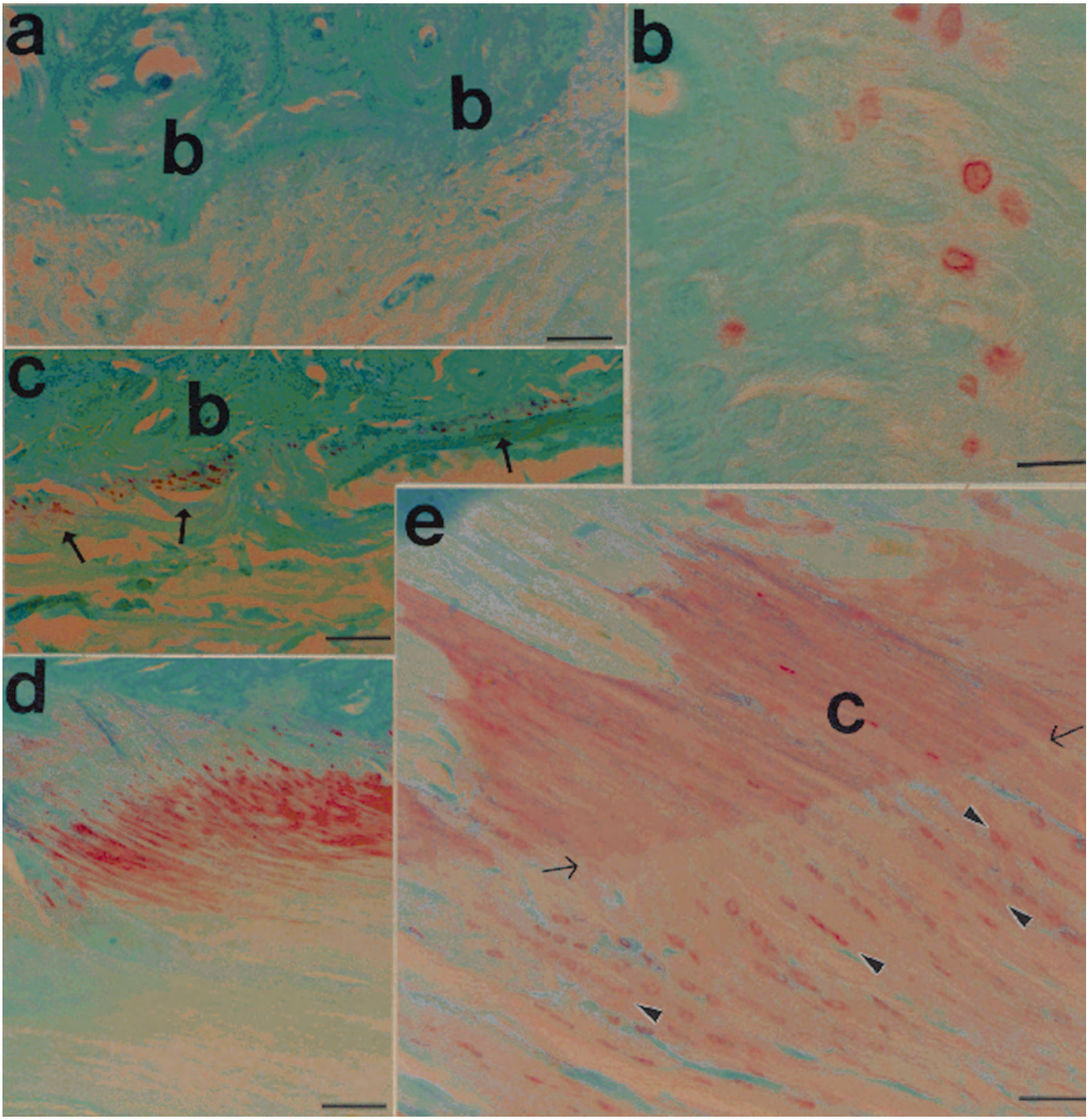

Fig. 18. Photomicrographs of tissue sections obtained from healthy feet of horses in the region of the DSIL-DDFT insertion of the distal phalanx. (A) Low magnification photomicrograph of tissues obtained from a 23-yr-old Dutch Warmblood did not reveal binding of safranin O dye to proteoglycan secretions. Bar = 80 ìm. (B) Higher magnification view of stressed tissues, revealing proteoglycan staining of cells with perinuclear cytoplasmic staining (red coloration) at the insertion site of the DSIL on the distal phalanx. Bar = 25 ìm. (C) Photomicrograph of tissues obtained from the region of the DSIL-DDFT insertion on the distal phalanx in a 6-yr-old Standardbred, revealing slight staining of proteoglycans. Bar = 300 ìm. (D) Photomicrograph of tissues obtained from a 6-yr-old Quarter Horse, revealing moderate staining with safranin O dye and mineralized cartilage between proteoglycan staining and bone in the insertion along the irregular border of the distal phalanx. Bar = 300 ìm. (E) High magnification photomicrograph revealing a tidemark (arrows) between the mineralized fibrocartilage insertion (c) and non-mineralized part of the DDFT and the DSIL with alignment of the fibroblasts in straight lines in lacunae (arrowheads). Notice the insertion site on the bone has an irregular surface shape. Arrowheads indicate fibroblasts that stained positive for proteoglycans. Bar = 80 ìm. For all panels, safranin O and fast green stains were used. Courtesy of *Am J Vet Res*.

rounded when they were inserted onto the distal phalanx flexor surface. Usually, there was a prominent mark (tidemark) that indicated the transition from non-mineralized connective tissue to the mineralized regions of the DSIL and the DDFT before its insertion onto the distal phalanx (Fig. 18E).[61] In these horses, the safranin O binding varied with a progressive increase in the proteoglycan staining of the fibroblasts and extracellular matrix in these connective tissues. Of this group of horses, little or no staining at the insertions of the DSIL and the DDFT occurred mainly in young horses under 5–6 yr (n = 13 horses) (Fig. 18A). When stain was evident, it was located perinuclearly in isolated cells with a small amount of stain in the extracellular matrix (Fig. 18B). With moderate staining, a greater number of cells had proteoglycan staining along the insertion of the DDFT and the DSIL that also extended proximally 1–2 mm from the attachments at the bony surface of the distal phalanx (n = 35 horses) (Fig. 18, C–E). Usually, a prominent tidemark was evident, which increased the width of the calcified cartilaginous portion of the insertion onto the bone. This widening of the calcified cartilage also revealed the response of the bone at the insertion, because it became a more roughened surface. In this small group of horses showing moderate staining, the age range was 4–22 yr, with a mean of 13 yr. In an older group of reasonably active horses, (i.e., ridden several times per week during the warmer months of the spring through the autumn) (n = 10 horses), the safranin O staining was slight with a few isolated cells along the insertion of the DSIL and the DDFT. In an additional group of race horses that died of catastrophic injury, the staining patterns ranged from no stains to moderate staining with no extensive staining patterns being evident to date.

In horses that were diagnosed with navicular syndrome (n = 10 horses), the safranin O staining along the insertion of the DSIL and the DDFT onto the flexor surface was greater in 8 of 10 specimens than compared with clinically sound horses. These horses had been diagnosed by different veterinarians from several practices in different states and had been treated several years (range, 3–8 yr) before being euthanized and donated to our laboratory. The staining patterns of the fibroblasts and extracellular matrix along the entire attachment of the DSIL and the DDFT had evidence of safranin O binding that extended several millimeters up to more than 10 mm from the distal phalanx proximally along the tendon and the DSIL (Fig. 19). In some specimens, small areas of cartilage were beginning to form within the DSIL and the dorsal half of the DDFT. The increased production of proteoglycans in tendons and ligaments occurs when the tissues are stressed by compressive forces.[63–68]

In other areas of the distal phalanx, morphological indications of stress[69–71] could also be seen, including in the articular cartilage of the joint between the navicular bone and the distal phalanx and on the articular cartilage of the navicular bone itself (Fig. 20). Using the safranin O stain that binds to proteoglycans, the articular cartilage stained a bright red coloration under "normal" or "unstressed" conditions. In the joint between the middle and the distal phalanx, the articular cartilage remained evenly stained throughout the entire histologic section and did not reveal any loss of safranin O staining. When there is a reduction or loss of binding of the safranin O dye within the articular cartilage, then less proteoglycan is present, which may indicate that the area does not function optimally in dissipating energy during movement and loads being applied to the joint surface.[64–65] In younger horses (usually under 4–6 yr), the joint between the navicular bone and the distal phalanx is usually homogeneously stained. However, in older horses, there is a progressive or gradual loss of binding beginning in the articular cartilage nearest the DSIL and progressing toward the joint surface between the middle and distal phalanx. These changes are evident in most horses. However, they are not strictly an age-related phenomenon, because navicular horses lose a greater amount of safranin O binding than older "normal" horses or horses without any clinical lameness problems.

In addition to the loss of proteoglycan staining, the duplication of tidemarks in the articular cartilage was noticeable in horses older than 4–6 yr. This means that the articular cartilage is being stressed by the loads applied to the foot of the horse, and the cartilage is adapting to the increased loads.[69–73] Tidemarks merely indicate the transition zone between the non-calcified and calcified cartilage within the articular cartilage. In most joints, there are usually one to two tidemarks normally present in the basal area of the cartilage when one progresses from the joint surface to the underlying bone.[69] One to two tidemarks were present in the cartilage between the middle and the distal phalanx. However, in most of the specimens greater than 7 yr, an increase in the number of tidemarks (duplication) was evident in the distal phalanx in the joint between the navicular bone and the distal phalanx, ranging upward of 10–12 tidemarks. The increasing numbers of tidemarks progressing toward the joint surface seemed to correlate with the decrease in proteoglycan staining. In the horses diagnosed with navicular syndrome, the relative number of tidemarks was slightly greater, usually 16–18 tidemarks.

Although these articular cartilage changes were evident in the distal phalanx as well as the navicular bone, other areas of changes in bone structure of the distal phalanx were also observed. In feet obtained from 50 horses, the microscopic structure and staining patterns of the trabecular and subchondral

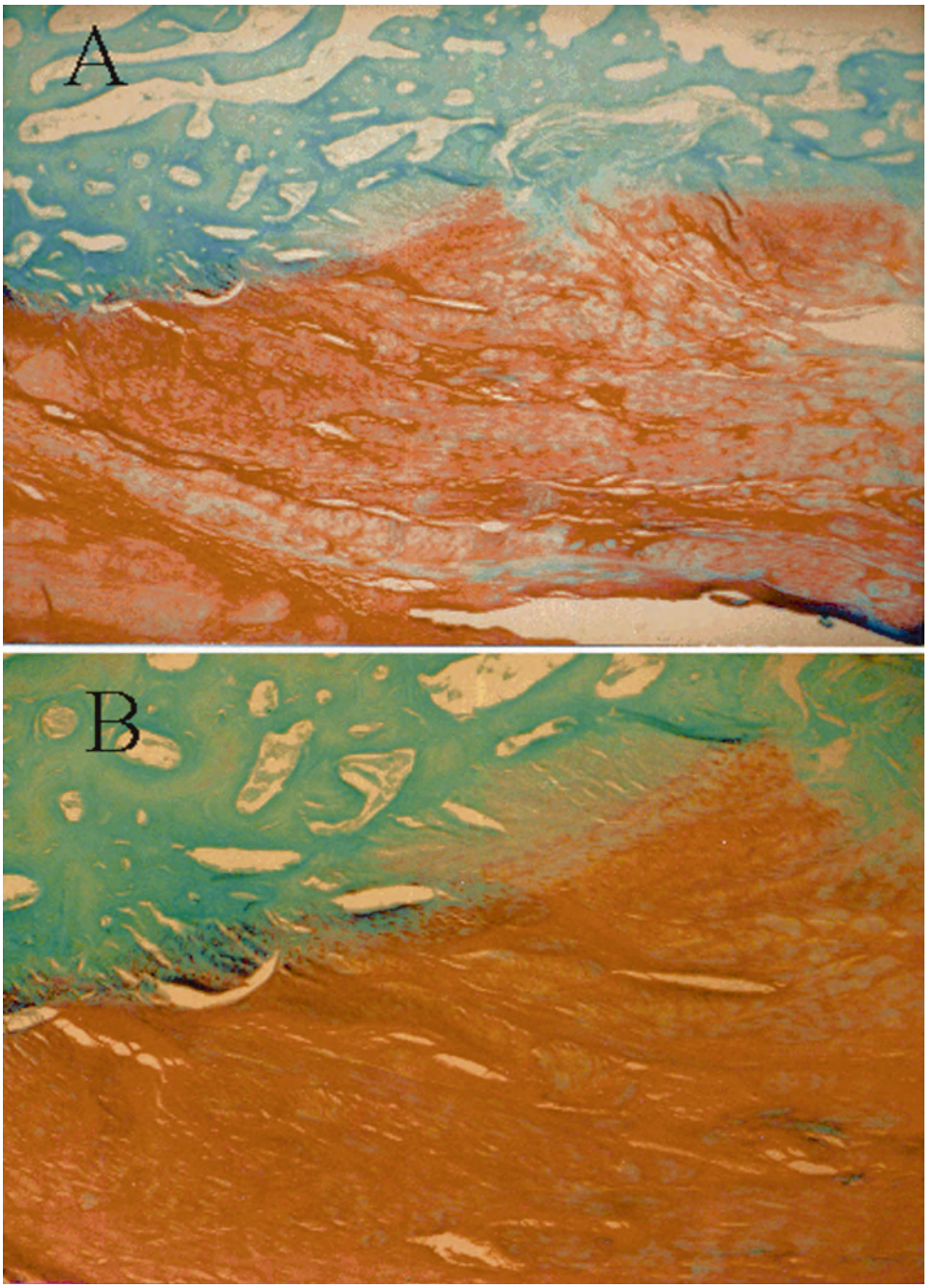

Fig. 19. In A, photomicrographs of the DSIL and DDFT insertion on distal phalanx in horse diagnosed with navicular syndrome showing extensive binding of increased proteoglycan staining. In B, higher power view of same horse showing extensive binding of safranin O. Compare with sections in Figure 18.

bone of the distal phalanx and navicular bone were determined from 3 to 10 slides from each site, using H&E (1–3 slides), toluidine blue (3–5 slides), and safranin O with fast green stain (2–3 slides). Sagittal sections of the distal phalanx and navicular bone were obtained at the articulation of the navicular bone and the distal phalanx. This sampling site represents the mediolateral extent of the articulation of the navicular bone with the distal phalanx and is located between the solar foramina. This region was selected, because the articulation between the navicular bone and the distal phalanx is greatest between the two solar foramen; however, the navicular bone extended further abaxially but did not usually form an articulation. The distal articulation of the middle phalanx was not ex-

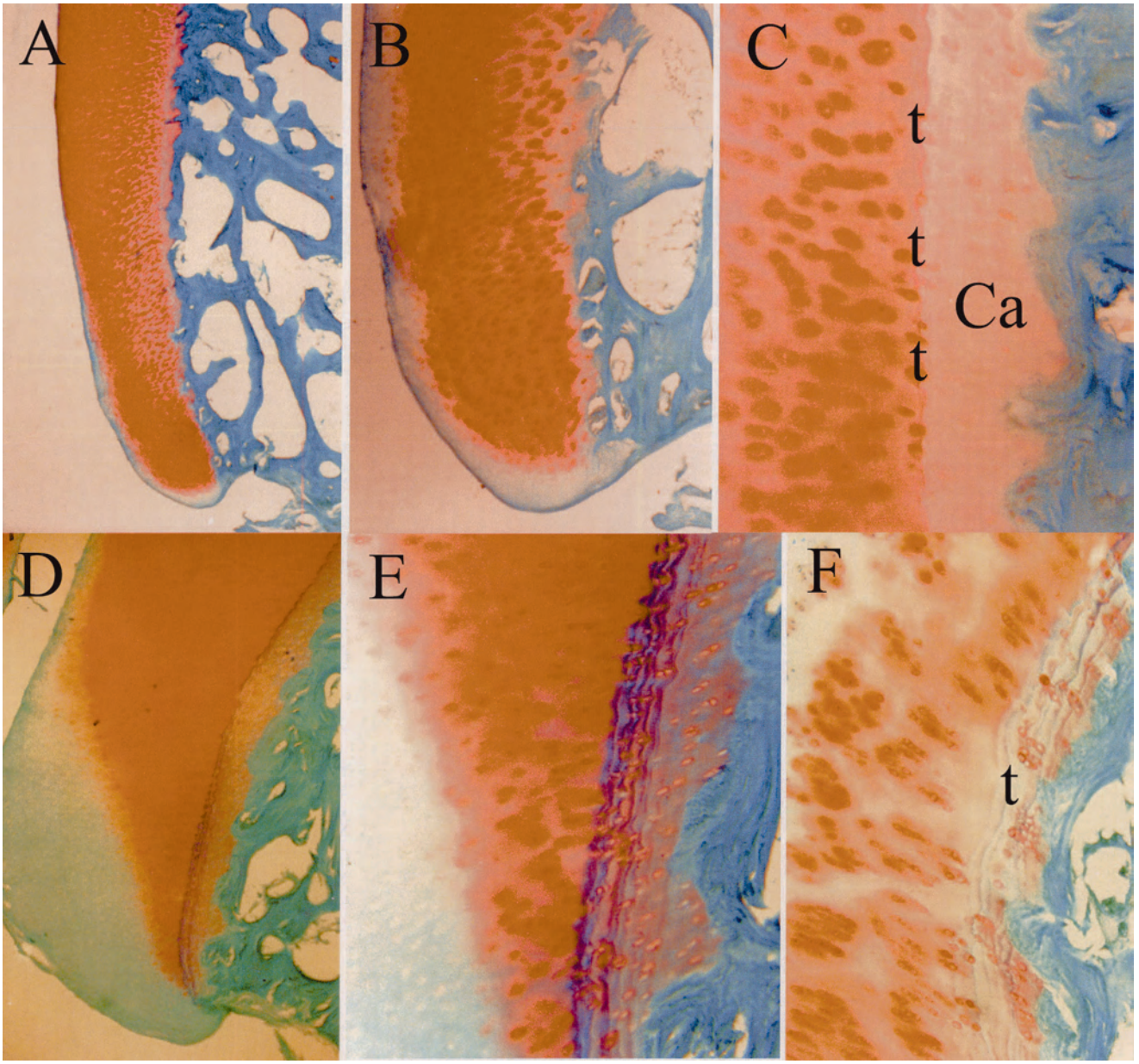

Fig. 20. Photomicrographs of distal phalanx in joint between navicular bone and distal phalanx. In young horse (top row), observe even stain of proteoglycan (A and B) with 1–2 tidemarks (t) in Ca-calcified cartilage. In bottom row, with increasing stress to joint, note the loss of staining (less red color) and the increase in tidemarks (t) in articular cartilage (D-F).

amined. All surfaces of the navicular bone were examined, whereas only the palmar two-thirds to three-fourths of the articular surface of the distal phalanx was examined microscopically because of the difficulty of embedding the entire joint surface in a tissue block.

Histomorphometry enabled the quantifications of the bone structures of this region of the distal phalanx in sound horses and navicular affected horses. The subchondral plate (SCP) in horses without any chronic foot problems of the distal phalanx at the attachments of the DSIL and the DDFT was 317.1 microns in young horses (<5 yr) with a progressive thinning to 278.6 microns in mature horses of 6–20 yr ($p < 0.05$). In older horses (>20 yr), the mean thickness was greater at 844.9 microns ($p < 0.05$). The trabecular thickness within the distal phalangeal bone was 169.2 microns, 161.7 microns, and 144.0 microns, respectively, for the three age groups. The relatively short length of SCP in the distal phalanx between the distal phalanx and the navicular bone (proximal to the DSIL and DDFT attachments) had a mean thickness of 475.0 microns with a range from 274.5 (>5 yr) to 637.9 microns. In the joint

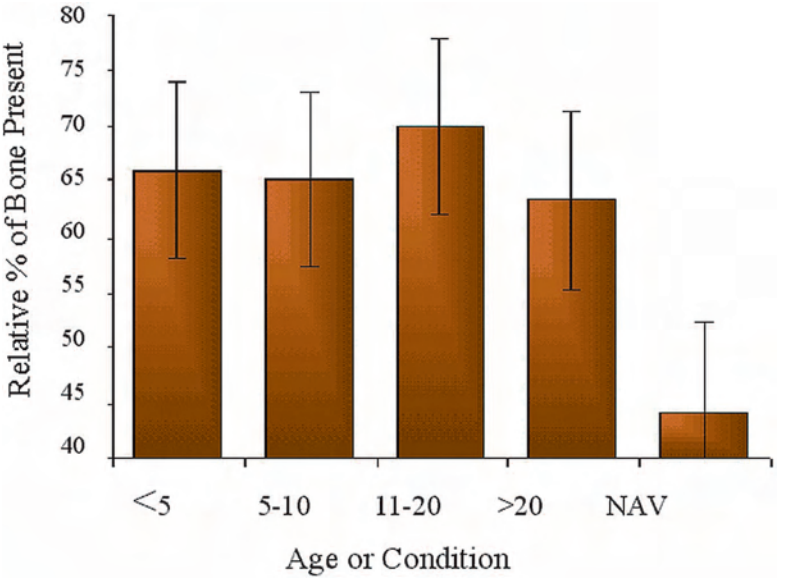

Fig. 21. Graph showing relative amount of bone area in different age groups (n = 39 horses) between 2 and 29 yr and navicular syndrome diagnosed horses. Note significant bone loss was observed in distal phalanx in latter group.

between the middle and distal phalanges, the SCP was relatively thick, ranging in thickness from 901.6 to 1505.5 microns. In the navicular bone of these healthy footed horses, the SCP had a mean thickness of 332.5 microns, whereas the trabecular thickness was 148.1 microns with a range of 156.5–137.6 microns for the respective age groups.

In horses diagnosed with navicular syndrome, the SCP at the attachments of the DSIL and the DDFT had a mean thickness of 260.8 microns, whereas between the distal phalanx and the navicular bone, the SCP was 185.5 microns. The trabecular bone thickness was 97.9 microns, regardless of the age. The SCP and the trabecular thickness were significantly thinner in navicular affected horses ($p < 0.05$). For the navicular bone, the SCP was 223.1 microns, and the trabecular thickness was 108.4 microns; both were thinner than the healthy footed horses ($p < 0.05$).

The relative percentage of bone within the distal phalanx of all healthy footed horses aged 2–31 yr was 66.1%. In those horses diagnosed with navicular syndrome, the bone area was 44.2%, which is significantly less ($p < 0.05$). The relative bone percent in the navicular bone was 60.7% for all age groups, whereas in the navicular affected horses, the percentage of bone was 43.9% ($p < 0.05$) (Figs. 21 and 22).

These latter observations show that there are definite morphological indicators of stress occurring in the DSIL, the DDFT, and the distal phalanx in the feet of healthy footed horses, and these tissues show significantly greater stress in those horses diagnosed with navicular syndrome. In the young horse with distal phalanges that were still growing, the SCP remains relatively thick at the attachments of the DSIL and the DDFT, because they are the internal supporting trabeculae of the distal phalanx.

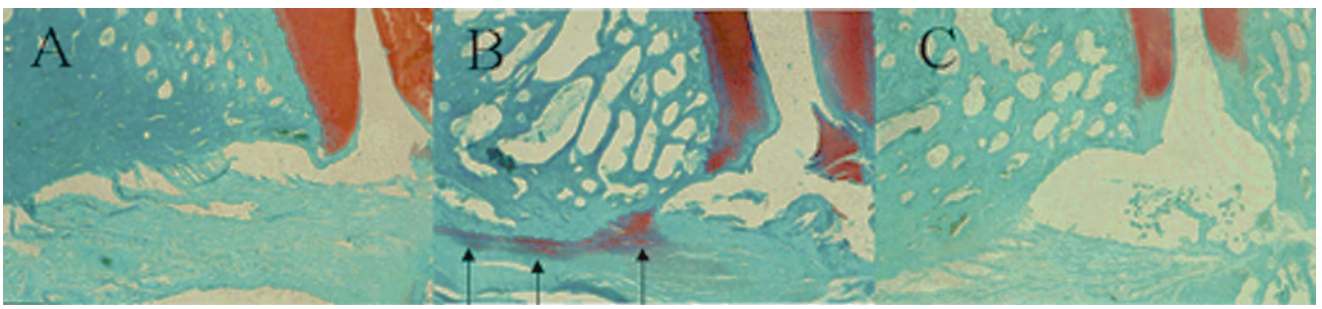

Fig. 22. Photomicrographs showing distal phalanx of a (A) young horse (6 yr), (B) navicular syndrome affected horse, and (C) older (25 yr) but active horse. Within the trabecular space of the distal phalanx, observe the osteopenia/osteoporosis of navicular affected horses. Black arrows indicate stress in the DSIL.

When an adult horse ages and adapts to its environment during stance and movement, the foot remodels with the distal phalanx undergoing several general changes including a progressive thickening of these SCPs and a slight thinning of the trabeculae. However, the relative percentage of bone remained unchanged within the distal phalanx. Within the navicular bone, similar changes were observed as the horse grows. In horses diagnosed with navicular syndrome, the changes within the navicular bone were significantly different from those of adult healthy footed horses with the trabeculae becoming significantly thinner and the relative amount of bone being much reduced. Within the distal phalanx, significant changes also occurred such as a thinning of the bone trabeculae and the SCP between the navicular bone and the distal phalanx. These two findings contributed to a significant loss of bone area in the distal phalanx to nearly one-third of that of healthy footed horses. These findings indicate that other areas, specifically the central and palmar parts of the distal phalanx, are structurally different in horses diagnosed with navicular syndrome and may contribute to the onset and persistence of the clinical signs of lameness.

This paper shows that the morphologies of the palmar foot and the distal phalanx are different in the feet of horses with healthy feet and horses with chronic lameness conditions. The lateral cartilage and the digital cushion in the palmar foot are underdeveloped in the horse affected by navicular syndrome when compared to a horse having few foot problems. The relative lack of support within the palmar foot (thin lateral cartilage and non-fibrocartilaginous digital cushion) may contribute to the usual appearance of the contracted heels and frog in horses with navicular syndrome. On the other hand, horses whose feet have extensive fibrocartilage within the digital cushion and thick lateral cartilage do not tend to have these foot problems. Further dorsally, the distal phalanx and the insertion sites of the DSIL and the DDFT seem to have fewer stress indicators in the feet of healthy horses than the feet of chronically lame horses. In these feet, there is less stress at the attachments, and the bone structure of the distal phalanx is more robust with greater thickness to the trabeculae and the subchondral plates. A greater area of bone is found in healthy feet than in those from navicular affected horses. In our opinion, these are demonstrable morphological indicators of stress occurring in the palmar foot and the distal phalanx. We believe that these changes occur over a long period of time with environmental influences being the major contributors to these changes. Environmental influences facilitate connective tissue stress and neurovascular control destruction, which in turn contributes to the osteopenia within the distal phalanx and the reported changes within the navicular bone.[29–34] With "proper foot stimulation" when the horse interacts within its environment during stance and movement, the foot adapts and becomes remodeled to form a "strong foot" as indicated above. However, in those feet without the "proper foot stimulation," the palmar foot and the distal phalanx may not be able to adapt and sufficiently change to protect themselves from the external stresses applied to the foot. These feet are not able to develop a "strong-footed" horse. In adult horses diagnosed with navicular syndrome, we believe that the palmar foot remains underdeveloped and there is a gradual loss of bone occurring within the distal phalanx leading to osteopenia. As a result, greater loads and stresses develop within the soft tissues of the foot (DSIL, DDFT, etc.) that can eventually lead to clinical signs of lameness. Although this hypothesis on the pathogenesis of navicular syndrome is simplistic, it is consistent with many of the pathological findings already published in veterinary literature.[29–36] However, it does suggest navicular syndrome is an "entire foot" problem and that other regions of the foot may be significant contributors to the onset of this disease process. Such a view broadens the current notion that the navicular bone is the primary and initiating focal point of the pathogenic process.

This study was supported in part by the American Quarter Horse Association, Grayson-Jockey Club Research Foundation, Inc., and Osha Products, Inc.

References and Footnotes

1. Stashak TS. The relationship between conformation and lameness. In: *Adams' Lameness in Horses*, 4th ed. Philadelphia: Lea & Febiger, 1987;71–79.
2. Ross MW. Conformation and lameness. In: Ross MW, Dyson SJ, eds. *Diagnosis and management of lameness in the horse.* Philadelphia: Saunders, 2003;15–31.
3. Parks A. The foot and shoeing. In: Ross MW, Dyson SJ, eds. *Diagnosis and management of lameness in the horse.* Philadelphia: Saunders, 2003;250–261.
4. Barrey E. Investigation of the vertical force distribution in the equine forelimb with an instrumented horseboot. *Equine Vet J* 1990;9(Suppl):35–38.
5. Ratzlaff MH, Grant BD, Frame JM, et al. Locomotor forces of galloping horses. In: Gillespie JR, Robinson NE, eds. *Equine exercise physiology II.* Davis, CA: ICEEP Publications, 1987;574–586.
6. Balch OK, Ratzlaff MH, Hyde ML, et al. Locomotor effects of hoof angle and mediolateral balance of horses exercising on a high-speed treadmill: preliminary results, in *Proceedings.* 37th Annual American Association of Equine Practitioners Convention 1991;687–708.
7. Pratt GW, O'Connor JT. Force plate studies of equine biomechanics. *Am J Vet Res* 1976;37:1251–1255.
8. Merkens HW, Schamhardt HC, Geertruda JVM, et al. Ground reaction force patterns of Dutch warmblood horses at normal trot. *Equine Vet J* 1993;25:134–137.
9. Dyhre-Poulsen P, Smedgaard HH, Roed J, et al. Equine hoof function investigated by pressure transducers inside the hoof and accelerometers mounted on the first phalanx. *Equine Vet J* 1994;26:362–366.
10. Leach DH, Dagg A. A review on equine locomotion and biomechanics. *Equine Vet J* 1983;15:93–102.
11. Nickel R, Schummer A, Seiferle E, et al. *The locomotor system of the domestic mammals.* Berlin: Verlag Paul Parey, 1986;444–466.

12. Bowker RM, Van Wulfen KK, Springer SE, et al. Functional anatomy of the cartilage of the distal phalanx and digital cushion in the equine foot and a hemodynamic flow hypothesis of energy dissipation. *Am J Vet Res* 1998;59:961–968.
13. Butler D. *The principles of horseshoeing II.* Maryville, Mo: Doug Butler Publisher, 1985;19–542.
14. Kainer RA. Functional anatomy of equine locomotor organs. In: Stashak TS, ed. *Adams' lameness in horses,* 4th ed. Philadelphia: Lea & Febiger, 1987;1–38.
15. Hickman J. *Farriery.* London: The structure and function of the foot. JA Allen, 1977;67–69.
16. Kainer RA. Clinical anatomy of the equine foot. *Vet Clin North Am [Equine Pract]* 1989;5:1–27.
17. Schummer A, Wilkins H, Vollmerhaus B, et al. *Circulatory system, skin and skin organs of the domestic mammals.* Berlin: Verlag Paul Parey, 1981;541–557.
18. Ratzlaff MH, Shindell RM, DeBowes RM. Changes in digital venous pressures of horses moving at the walk and trot. *Am J Vet Res* 1985;46:1545–1549.
19. Goshal NG, Venous drainage of the thoracic and pelvic limbs. In: Goshal NG, Koch T, Popesko P. *Venous drainage of the domestic animals.* Philadelphia: WB Saunders Co, 1981; 167–172.
20. Sack WO. *Rooney's guide to the dissection of the horse,* 6th ed. Ithaca: Veterinary Textbooks, 1994;134–152.
21. Schummer A. Blutgefabe und Zirkulationsverhaltnisse im Zehenendorgan des Pferdes. *Morph Jb* 1951;91:568–649.
22. Barrey E, Landjerit B, Wollter R. Shock and vibration during the hoof impact on different tract surfaces. In: Persson SG, Lindholm A, Jeffcott LB, eds. *Equine exercise physiology.* Davis, CA: ICEEP Publications, 1991;97–106.
23. Simon SR, Paul IL, Mansour J, et al. Peak dynamic force in human gait. *J Biomech* 1981;14:817–822.
24. Milnor WR. Principles of hemodynamics. In: Mountcastle VB, ed. *Medical physiology.* St. Louis: CV Mosby Co, 1980;1017–1032.
25. Light LH, McLellan GE, Klernerman L. Skeletal transients on heel strike in normal walking with different footware. *J Biomech* 1980;13:477–480.
26. Radin EL, Parker HG, Pugh JW, et al. Response of joints to impact loading. III. Relationship between trabecular microfractures and cartilage degeneration. *J Biomech* 1973;6:51–57.
27. Bowker RM, Brewer AM, Vex KB, et al. Sensory receptors in the equine foot. *Am J Vet Res* 1993;54:1840–1844.
28. Stashak TS. Lameness. In: Stashak TS, ed. *Adams' lameness in horses.* Philadelphia: Lea & Febiger, 1987; 486–568.
29. Pool RR, Meagher DM, Stover SM. Pathophysiology of navicular syndrome. *Vet Clin North Am [Equine Pract]* 1989; 5:109–144.
30. MacGregor CM. Navicular disease–in search of definition. *Equine Vet J* 1989;21:389–391.
31. Meier HP. A review of investigations of etiology of navicular disease. In: Hertsch B, ed. *International symposium on podotroclosis.* Munich: FN-Verlag der Deutschen Reiterlichen Vereinigung, 1994;57–59.
32. Dyson SJ. Navicular disease and other soft tissue causes of palmar foot pain. In: Ross MW, Dyson SJ, eds. *Diagnosis and management of lameness in the horse.* Philadelphia: Saunders, 2003;286–299.
33. Wright IM, Kidd L, Thorp BH. Gross, histological and histomorphometric features of the navicular bone and related structures in the horse. *Equine Vet J* 1998;30:220–234.
34. Ostblom L, Lund C, Melsen F. Histological study of navicular bone disease. *Equine Vet J* 1982;14:199–202.
35. Van Wulfen KK, Bowker RM. Microanatomic characteristics of the insertion of the distal sesamoideum impar ligament and deep digital flexor tendon on the distal phalanx in healthy feet obtained from horses. *Am J Vet Res* 2002;63: 215–221.
36. Bowker RM, Van Wulfen KK. Microanatomy of the intersection of the distal sesamoideum impar ligament and the deep digital flexor tendon: A preliminary report. *Pferdeheikunde* 1996;12:623–627.
37. Bowker RM, Atkinson PJ, Atkinson TS, et al. Effect of contact stress in bones of the distal interphalangeal joint on microscopic changes in articular cartilage and ligaments. *Am J Vet Res* 2001;62:414–424.
38. Atkinson TS, Haut RC, Attiero NJ. A poroelastic model that predicts some phenomenological responses of ligaments and tendons. *J Biomech Eng* 1997;119:400–405.
39. Schryver HF, Bartel DL, Langrana N, et al. Locomotion in the horse: kinematics and external and internal forces in the normal equine digit in the walk and trot. *Am J Vet Res* 1978;39:1728–1733.
40. Riemersma DJ, Bogert AJ, Jansen MO, et al. Tendon strain in the forelimbs as a functional gait and ground characteristics and in vitro limb loading in ponies. *Equine Vet J* 1996; 28:133–138.
41. Lochner FK, Milne DN, Mills E. In vivo and in vitro measurement of tendon strain in the horse. *Am J Vet Res* 1980; 41:1929–1937.
42. Rijkenhuizen A, Nemeth F, Dik K, et al. The arterial supply of navicular bone in the normal horse. *Equine Vet J* 1989; 21:399–404.
43. Williams PL, Warwick R, Dyson M, et al. Myology. In: Williams PL, Warwick R, Dyson M, et al, eds. *Gray's anatomy,* 37th ed. New York: Churchill Livingstone, 1989; 563–565.
44. Molyneux GS, Haller CJ, Mogg K, et al. The structure, innervation and location of arteriovenous anastomoses in the equine foot. *Equine Vet J* 1994;26:305–312.
45. Pollock DC, Li Z, Koman LA, et al. Control of arteriovenous anastomoses in rabbit ear model of digital perfusion. *Am J Physiol* 1996;271:H2007–H2013.
46. Zhongyu L, Komar A, Smith BP. Alpha adrenoceptors in the rabbit ear thermoregulatory microcirculation. *Cardiovasc Res* 1998;55:115–123.
47. Kimball ES. Substance P, cytokines, and arthritis. *Ann NY Acad Sci* 1990;594:293–308.
48. Taylor DCM, Pierau FK. *Nociceptive afferent neurons.* New York: Manchester University Press, 1991;18–35,50–66.
49. Uddmann R, Edvinsson L, Ekblad E, et al. Calcitonin gene-related peptide [CGRP]: perivascular distribution of vasodilatory effects. *Regul Pept* 1986;15:1–23.
50. Bowker RM, Rockershouser SJ, Linder K, et al. A silver-impregnation and immunocytochemical study of innervation of the distal sesamoid bone and its suspensory ligaments in the horse. *Equine Vet J* 1994;26:212–219.
51. Weihe E. Neuropeptides in primary afferent neurons. In: Zenker W, Neuhuber WK, eds. *The primary afferent neuron.* New York: Plenum Press, 1990;127–159.
52. Moncada S, Palmer RM, Higgs EA. Nitric oxide: physiology, pathophysiology, and pharmacology. *Pharmacol Rev* 1991;43:109–142.
53. Farrell DM, Biship VS. Permissive role of nitric oxide in active theromoregulatory vasodilation in rabbit ear. *Am J Physiol* 1995;269:H1613–H1618.
54. Mantyh P, Catton MD, Boehmer CG, et al. Receptors of sensory neuropeptides in human inflammatory disease: implications for the effector role of sensory neurons. *Peptides* 1989;10:627–645.
55. Gamse R, Saria A. Potentiation of tachykinin-induced plasma protein extravasation by calcitonin gene-related peptide. *Eur J Pharmacol* 1985;114:61–66.
56. Mantyh PW, Gates T, Mantyh CR, et al. Autoradiographic localization and characterization of tachykinin receptor binding sites in the rat brain and peripheral tissue. *J Neurosci* 1989;9:258–279.
57. Van Wulfen KK, Bowker RM. Evaluation of tachykinins and their receptors to determine sensory innervation in the dorsal hoof wall and insertion of the distal sesamoideum impar ligament and deep digital flexor tendon on the distal

phalanx in healthy feet of horses. *Am J Vet Res* 2002;63: 222–228.
58. Burn JF, Wilson A, Nason GP. Impact during equine locomotion: techniques for measurement and analysis. *Equine Vet J* 1997;23(Suppl):9–12.
59. Schamhardt HC, Merkens HW. Objective determination of ground contact of equine limbs at the walk and trot: comparison between ground reaction forces, accelerometer data and kinematics. *Equine J Vet* 1994;17(Suppl):75–79.
60. Ratzlaff MH, Hyde ML, Grant BD, et al. Measurement of vertical forces and temporal components of the strides of horses using instrumented boots. *Equine Vet Sci* 1990;10: 23–25.
61. Cooper RR, Misol S. Tendon and ligament insertion. A light and electron microscopic study. *J Bone Joint Surg Am* 1970;52:1–20.
62. Benjamin J, Evans EJ, Copp L. The histology of tendon attachments to bone in man. *J Anat* 1986;149:89–100.
63. Matyas JR, Antow MG, Shrive NG, et al. Stress governs tissue phenotype at the femoral insertion of the rabbit MCL. *J Biomech* 1995;28:147–157.
64. Vogel KG, Ordras A, Pogany G, et al. Proteoglycans in the compressed region of the human tibialis posterior tendon and in ligaments. *J Orthop Res* 1993;11:68–77.
65. Gillard G, Reilly HC, Bell-Both PG, et al. The influence of mechanical forces on the glycosaminoglycan content of the rabbit flexor digitorum profundus tendon. *Connect Tissue Res* 1979;7:37–46.
66. Woo SL, Gomez MA, Sites TJ, et al. The biomechanical and morphological changes in the medial collateral ligament of the rabbit after immobilization and remobilization. *J Bone Joint Surg Am* 1987;69:1200–1211.
67. Giori NJ, Beaure GS, Carter DR. Cellular shape and pressure may mediate mechanical control of tissue composition in tendons. *J Orthop Res* 1993:11;581–591.
68. Vogel KG, Koob TJ. Structural specialization in tendons under compression. *Int Rev Cytol* 1989;115:267–293.
69. Redler I, Mow VC, Zimny ML, et al. The ultrastructure and biomechanical significance of the tidemark of articular cartilage. *Clin Orthop* 1975;112:357–362.
70. Mow VC, Kwaw MK, Lai WM. Fluid transport and mechanical properties of articular cartilage: a review. *J Biomech* 1984;17:377–394.
71. Radin EL, Rose RM. Role of subchondral bone in the initiation and progression of cartilage damage. *Clin Orthop* 1986;213:34–40.
72. Vener MJ, Thompson RC, Lewis JL, et al. Subchondral bone damage after acute transarticular loading. An in vitro model of joint injury. *J Orthop Res* 1992;10:759–765.
73. Newberry W, Zukosky D, Haut R. Subfracture insult to a knee joint causes alterations in the bone and in the functional stiffness of the overlying cartilage. *J Orthop Res* 1997;15: 450–455.

[a]Bowker RM, Natchek KA. Age and breed differences of the palmar foot. *Am J Vet Res* (in press).
[b]Bowker RM, Kalck KA, VanWulfen KK. Morphological indicators of stress in the foot of normal and navicular diagnosed horses. *Am J Vet Res* (in press).